AIChE

Guaranteed Cost Distributed Fuzzy Observer-Based Control for a Class of Nonlinear Spatially Distributed Processes

Jun-Wei Wang and Huai-Ning Wu
Science and Technology on Aircraft Control Laboratory, School of Automation Science and Electrical Engineering, Beihang University (Beijing University of Aeronautics and Astronautics), Beijing 100191, P.R. China

Han-Xiong Li
Dept. of Systems Engineering and Engineering Management, City University of Hong Kong, Kowloon, Hong Kong SAR

DOI 10.1002/aic.14001
Published online January 30, 2013 in Wiley Online Library (wileyonlinelibrary.com)

The guaranteed cost distributed fuzzy (GCDF) observer-based control design is proposed for a class of nonlinear spatially distributed processes described by first-order hyperbolic partial differential equations (PDEs). Initially, a T–S fuzzy hyperbolic PDE model is proposed to accurately represent the nonlinear PDE system. Then, based on the fuzzy PDE model, the GCDF observer-based control design is developed in terms of a set of space-dependent linear matrix inequalities. In the proposed control scheme, a distributed fuzzy observer is used to estimate the state of the PDE system. The designed fuzzy controller can not only ensure the exponential stability of the closed-loop PDE system but also provide an upper bound of quadratic cost function. Moreover, a suboptimal fuzzy control design is addressed in the sense of minimizing an upper bound of the cost function. The finite difference method in space and the existing linear matrix inequality optimization techniques are used to approximately solve the suboptimal control design problem. Finally, the proposed design method is applied to the control of a nonisothermal plug-flow reactor. © 2013 American Institute of Chemical Engineers *AIChE J*, 59: 2366–2378, 2013

Keywords: guaranteed cost control, distributed parameter systems, Takagi–Sugeno fuzzy model, exponential stability, linear matrix inequalities

Introduction

The behavior of most chemical processes must depend on spatial position and time, such as heat conduction, fluid flow, and chemical reactor processes.[1–3] The mathematical models of these processes usually take the form of partial differential equations (PDEs) and are often derived from the fundamental balances of momentum, energy, and material. Moreover, these processes are nonlinear in nature. In such a situation, the investigations on the control synthesis for nonlinear PDE systems are of theoretical and practical importance. According to the properties of the spatial differential operator (SDO), the PDE systems can be generally classified into hyperbolic, parabolic, elliptic, and so forth.[1] The type of PDE systems essentially determines the approaches for solving the control problem for PDE systems.

For a parabolic PDE system, the fact that the system dynamics is practically determined by a finite number of modes, motivates the use of modal decomposition techniques (predominantly Galerkin's method) to derive a low-dimensional ordinary differential equation (ODE) models that capture the dominant dynamics of the systems,[4–8] which is then used for control design purposes. The recent development using finite-dimensional approximation includes linear quadratic (LQ) optimal control[9] and robust fuzzy observer-based control[10] based on ODEs derived from the standard Galerkin method, reconfiguration-based fault-tolerant control,[11] and constrained H_∞ fuzzy observer-based control[12] on the basis of ODEs obtained from the singular perturbation formulation of Galerkin's method. In contrast to parabolic PDE systems, hyperbolic PDE systems involve an SDO whose eigenvalues cluster along vertical or nearly vertical asymptotes in the complex plane and thus cannot be accurately represented by a finite number of modes. These systems can represent the dynamics of industrial processes involved in convection with negligible diffusion effects, for example, fluid heat exchanger, plug-flow reactor (PFR), and fixed-bed reactor.[1] Having recognized that the space-distributed nature of hyperbolic PDE systems has to be included in the control development, some control approaches have been proposed, for example, LQ optimal control,[1,13,14] sliding mode control,[15] geometric control,[2,16,17] and model predictive control.[18–20] Despite these promising efforts, however, the control of nonlinear hyperbolic PDE systems is a broad area, and further research is required to develop a simple and effective control methodology.

In the past few years, many authors have devoted considerable effort to develop various feasible approaches to solve

Correspondence concerning this article should be addressed to H.-N. Wu at whn@buaa.edu.cn.

the problems of stability analysis and synthesis of nonlinear systems. Among these approaches, fuzzy control based on Takagi–Sugeno (T–S) fuzzy model[21] becomes more and more popular (see e.g., Refs. 22–24 and the references therein for a survey of recent development), as it can combine the merits of both fuzzy logic theory and linear system theory. It has been shown that fuzzy logic theory is one of the most useful techniques for utilizing qualitative, linguistic information about a highly complex nonlinear system to decompose the task of modeling and control design into a group of easier local tasks. At the same time, it also provides the mechanism to blend these local tasks together to yield the overall model and control design. On the other hand, advances in linear system theory have made a large number of powerful design tools available. As a consequence, based on the T–S fuzzy model, the fruitful linear system theory can be applied to the stability analysis and controller synthesis of nonlinear systems. As a common belief, this fuzzy-model-based control technique is conceptually simple and effective for controlling complex nonlinear systems. So far, many effective control methods have been reported for nonlinear systems represented by the T–S fuzzy model.[25–30] However, the existing fuzzy-model-based results are mainly developed for nonlinear ODE systems. More recently, Wang et al.[31] developed a distributed fuzzy exponential stabilizing control design method for a class of nonlinear hyperbolic PDE systems. Yet, the result[31] only considers a simple stabilization problem and requires that the complete information of the state variables of the PDE system is available.

Motivated by the aforementioned considerations, this study will deal with the guaranteed cost distributed fuzzy (GCDF) observer-based control design problem for a class of nonlinear hyperbolic PDE systems. By using the T–S fuzzy PDE modeling method and the parallel distributed compensation (PDC) scheme,[22] a distributed fuzzy observer-based controller is developed such that the closed-loop PDE system is exponentially stable and an upper bound of quadratic cost function is provided. In our control scheme, a distributed fuzzy observer is proposed to estimate the state of the PDE system. The outcome of the GCDF observer-based control problem is presented in terms of a set of space-dependent linear matrix inequalities (SDLMIs). Moreover, a suboptimal control design problem is addressed in the sense of minimizing an upper bound of the cost function, which is simply formulated as an SDLMI-based minimization problem. The minimization problem can be solved approximately using the finite difference method in space and the existing linear matrix inequality (LMI) optimization techniques.[32,33] Finally, the developed design method is successfully applied to the control of a nonisothermal PFR. It is worth emphasizing that this study addresses a fuzzy observer-based control design with an optimized guaranteed cost, which is different from the one[31] where a simple fuzzy state feedback stabilizing control design was only given.

Briefly, the rest of this article is organized as follows. "Fuzzy PDE Modeling and Problem Formulation" section introduces the problem formulation. "GCDF Observer-Based Control Design" section presents a GCDF observer-based control design method via SDLMIs and an LMI algorithm is proposed to approximately solve the SDLMI optimization problem. In "Simulation Example" section, the application of the proposed design method to a nonisothermal PFR is provided to illustrate its effectiveness. Finally, some concluding remarks are offered in "Conclusions" section.

Notations

The following notations will be used throughout this article. $\Re$, $\Re^n$, and $\Re^{m\times n}$ denote the set of all real numbers, n-dimensional Euclidean space, and the set of all $m \times n$ matrices, respectively. $\|\cdot\|$ and $\langle \cdot,\cdot\rangle_{\Re^n}$ denote the Euclidean norm and inner product for vectors, respectively. Identity matrix, of appropriate dimensions, will be denoted by $\boldsymbol{I}$. For a real square matrix $\boldsymbol{M}$ and $\boldsymbol{M}>0$ ($\boldsymbol{M}<0$ and $\boldsymbol{M}\leq 0$, respectively) means that $\boldsymbol{M}$ is symmetric and positive definite (negative definite and negative semidefinite, respectively). The real square space-varying matrix function $\boldsymbol{P}(x)$, $x \in [z_1, z_2]$ is symmetric and positive definite (negative definite and negative semidefinite, respectively), if $\boldsymbol{P}(x)>0$ ($\boldsymbol{P}(x)<0$ and $\boldsymbol{P}(x)\leq 0$, respectively) for each $x \in [z_1, z_2]$. $\lambda_{\min}$ ($\boldsymbol{A}$) and $\lambda_{\max}$ ($\boldsymbol{A}$) mean the minimum and maximum eigenvalues of a real square matrix $\boldsymbol{A}$, respectively. $\mathscr{H}^n = \mathscr{Q}_2([z_1, z_2]; \Re^n)$ is an Hilbert space of n-dimensional square integrable vector functions $\boldsymbol{\omega}(x) \in \Re^n$ and $x \in [z_1, z_2] \subset \Re$ with the inner product and norm

$$\langle \boldsymbol{\omega}_1, \boldsymbol{\omega}_2 \rangle = \int_{z_1}^{z_2} \langle \boldsymbol{\omega}_1(z), \boldsymbol{\omega}_2(z) \rangle_{\Re^n} dz \text{ and } \|\boldsymbol{\omega}_1\|_2 = \langle \boldsymbol{\omega}_1, \boldsymbol{\omega}_1 \rangle^{1/2}$$

where $\boldsymbol{\omega}_1$ and $\boldsymbol{\omega}_2 \in \mathscr{H}^n$. The superscript "$T$" is used for the transpose of a vector or a matrix.

Fuzzy PDE Modeling and Problem Formulation

We consider nonlinear first-order hyperbolic PDE systems in one spatial dimension with a state-space description of the following form

$$\frac{\partial \boldsymbol{y}(x,t)}{\partial t} = \theta(x)\frac{\partial \boldsymbol{y}(x,t)}{\partial x} + \boldsymbol{f}(\boldsymbol{y}(x,t),x) + \boldsymbol{G}(\boldsymbol{y}(x,t),x)\boldsymbol{u}(x,t) \quad (1)$$

$$\boldsymbol{y}_c(x,t) = \boldsymbol{h}_c(\boldsymbol{y}(x,t),x) \quad (2)$$

$$\boldsymbol{z}(x,t) = \boldsymbol{h}_z(\boldsymbol{y}(x,t),x) + \boldsymbol{D}(\boldsymbol{y}(x,t),x)\boldsymbol{u}(x,t) \quad (3)$$

subject to the boundary condition

$$\boldsymbol{E}_1\boldsymbol{y}(z_1,t) + \boldsymbol{E}_2\boldsymbol{y}(z_2,t) = \boldsymbol{d}(t) \quad (4)$$

and the initial condition

$$\boldsymbol{y}(x,0) = \boldsymbol{y}_0(x)$$

where $\boldsymbol{y}(x,t) \in \Re^n$ denotes the state, $x \in [z_1, z_2] \subset \Re$ and $t \in [0, \infty)$ denote position and time, respectively, $\boldsymbol{u}(x,t) \in \Re^m$ stands for the control input, $\boldsymbol{y}_c(x,t) \in \Re^p$ is the measured output, and $\boldsymbol{z}(x,t) \in \Re^q$ denotes the controlled output. $\boldsymbol{f}(\boldsymbol{y}(x,t),x)$, $\boldsymbol{G}(\boldsymbol{y}(x,t),x)$, $\boldsymbol{h}_c(\boldsymbol{y}(x,t),x)$, $\boldsymbol{h}_z(\boldsymbol{y}(x,t),x)$, and $\boldsymbol{D}(\boldsymbol{y}(x,t),x)$ are locally Lipschitz continuous in $\boldsymbol{y}(x, t)$ with appropriate dimensions and $\boldsymbol{f}(\boldsymbol{y}(x,t),x)$, $\boldsymbol{h}_c(\boldsymbol{y}(x,t),x)$ satisfies $\boldsymbol{f}(0,x)=0$, $\boldsymbol{h}_c(0,x)=0$, for all $x \in [z_1, z_2]$. $\theta(x)$ is a real known scalar function of x, and $\boldsymbol{E}_1$ and $\boldsymbol{E}_2$ are real known matrices with appropriate dimensions. $\boldsymbol{d}(t)$ is assumed to be a C^1 continuous function of time, that is, both $\boldsymbol{d}(t)$ and its derivative function are continuous with respect to t, $\boldsymbol{y}_0(x) \in \Re^n$ is a known initial state. Furthermore, the boundary condition in Eq. 4 is more general and captures the possibility that the system of Eqs. 1–3 may admit boundary conditions at two separate points and periodic boundary conditions.

For simplicity, when $\boldsymbol{u}(x,t) \equiv 0$, the system of Eq. 1 is referred to as an "unforced" system. We introduce the following definition of exponential stability on Hilbert space $\mathscr{H}^n$:

Definition 1. The unforced system of Eq. 1 (i.e., $\boldsymbol{u}(x,t)\equiv 0$) is said to be "exponentially stable," if there exist positive scalars ϑ, ς, and v such that $\|\boldsymbol{y}(\cdot,t)\|_2^2 < \varsigma\|\boldsymbol{y}_0(\cdot)\|_2^2 \exp(-vt)$, for $\forall t\geq 0$ and $\|\boldsymbol{y}_0(\cdot)\|_2^2 < \vartheta$.

In this article, the nonlinear hyperbolic PDE system of Eqs. 1–4 is assumed to be exactly represented by the following T–S fuzzy PDE model described by fuzzy IF–THEN rules, which express local dynamics using a linear hyperbolic PDE model:

Plant Rule i:
IF $\xi_1(x,t)$ is F_{i1} and … and $\xi_l(x,t)$ is F_{il}

$$\textbf{THEN}\begin{cases}\partial \boldsymbol{y}(x,t)/\partial t=\boldsymbol{A}\boldsymbol{y}(x,t)+\boldsymbol{A}_i(x)\boldsymbol{y}(x,t)+\boldsymbol{G}_i(x)\boldsymbol{u}(x,t)\\ \boldsymbol{y}_c(x,t)=\boldsymbol{C}_i(x)\boldsymbol{y}(x,t)\\ z(x,t)=\boldsymbol{H}_i(x)\boldsymbol{y}(x,t)+\boldsymbol{D}_i(x)\boldsymbol{u}(x,t),\quad i\in\mathcal{S}\triangleq\{1,2,\cdots,r\}\end{cases}\tag{5}$$

where F_{ij}, $i\in\mathcal{S}$, $j=1,2,\ldots,l$ are fuzzy sets, $\boldsymbol{A}$ is an SDO defined as $\boldsymbol{A}\boldsymbol{y}(x,t)=\theta(x)\partial\boldsymbol{y}(x,t)/\partial x$, and $\boldsymbol{A}_i(x)$, $\boldsymbol{G}_i(x)$, $\boldsymbol{C}_i(x)$, $\boldsymbol{H}_i(x)$, and $\boldsymbol{D}_i(x)$ for $i\in\mathcal{S}$ are real known matrix functions with appropriate dimensions, r is the number of IF–THEN rules. $\xi_1(x,t)$–$\xi_l(x,t)$ are the premise variables that are assumed to be functions of both available state variables and spatial variable in this study. It has been shown that an exact T–S fuzzy ODE model construction from a given nonlinear dynamical ODE model can be obtained by the sector nonlinearity approach.[22] Applying this approach to the nonlinear hyperbolic PDE system of Eqs. 1, we can also obtain an exact T–S fuzzy hyperbolic PDE model construction.

By applying the center-average defuzzifier, product interference, and singleton fuzzifier, the overall dynamics of T–S fuzzy PDE system of Eq. 5 can be expressed as

$$\begin{aligned}\frac{\partial \boldsymbol{y}(x,t)}{\partial t}&=\boldsymbol{A}\boldsymbol{y}(x,t)+\sum_{i=1}^{r}h_i(\xi(x,t))[\boldsymbol{A}_i(x)\boldsymbol{y}(x,t)+\boldsymbol{G}_i(x)\boldsymbol{u}(x,t)]\\ &=\boldsymbol{A}\boldsymbol{y}(x,t)+\boldsymbol{A}(\xi,x)\boldsymbol{y}(x,t)+\boldsymbol{G}(\xi,x)\boldsymbol{u}(x,t)\end{aligned}\tag{6}$$

$$\boldsymbol{y}_c(x,t)=\sum_{i=1}^{r}h_i(\xi(x,t))\boldsymbol{C}_i(x)\boldsymbol{y}(x,t)=\boldsymbol{C}(\xi,x)\boldsymbol{y}(x,t)\tag{7}$$

$$\begin{aligned}\boldsymbol{z}(x,t)&=\sum_{i=1}^{r}h_i(\xi(x,t))[\boldsymbol{H}_i(x)\boldsymbol{y}(x,t)+\boldsymbol{D}_i(x)\boldsymbol{u}(x,t)]\\ &=\boldsymbol{H}(\xi,x)\boldsymbol{y}(x,t)+\boldsymbol{D}(\xi,x)\boldsymbol{u}(x,t)\end{aligned}\tag{8}$$

where $\xi(x,t)=[\xi_1(x,t)\ \ldots\ \xi_l(x,t)]^T$ and

$$\boldsymbol{M}(\xi,x)=\sum_{i=1}^{r}h_i(\xi(x,t))\boldsymbol{M}_i(x),$$
$$\boldsymbol{M}_i(\cdot)\in\{\boldsymbol{A}_i(\cdot),\boldsymbol{G}_i(\cdot),\boldsymbol{C}_i(\cdot),\boldsymbol{H}_i(\cdot),\boldsymbol{D}_i(\cdot)\},$$
$$w_i(\xi(x,t))=\prod_{j=1}^{l}F_{ij}(\xi_j(x,t)),$$
$$h_i(\xi(x,t))=w_i(\xi(x,t))/\sum_{i=1}^{r}w_i(\xi(x,t)),\quad i\in\mathcal{S}$$

$F_{ij}(\xi_j(x,t))$ is the grade of the membership of $\xi_j(x,t)$ in F_{ij}, for $i\in\mathcal{S}$. In this article, it is assumed that

$$w_i(\xi(x,t))\geq 0,\quad i\in\mathcal{S},\qquad\text{and}\quad \textstyle\sum_{i=1}^{r}w_i(\xi(x,t))>0$$

for all $x\in[z_1,z_2]$ and $t\geq 0$. Then, we can obtain the following conditions

$$h_i(\xi(x,t))\geq 0,\quad i\in\mathcal{S},\quad\text{and}\quad \sum_{i=1}^{r}h_i(\xi(x,t))=1$$

for all $x\in[z_1,z_2]$ and $t\geq 0$.

More recently, a distributed fuzzy state feedback controller has been proposed to exponentially stabilize nonlinear hyperbolic PDE system.[31] In real-world control problems, however, it is often the case that the complete information of the state variables of a system is not always available. In this situation, one needs to resort to output feedback design methods such as observer-based designs. In this article, the following fuzzy observer is proposed to deal with the state estimation of the system of Eqs. 1–4:

Observer Rule i:
IF $\xi_1(x,t)$ is F_{j1} and … and $\xi_l(x,t)$ is F_{jl}

$$\begin{aligned}\textbf{THEN}\ \frac{\partial\hat{\boldsymbol{y}}(x,t)}{\partial t}&=\boldsymbol{A}\hat{\boldsymbol{y}}(x,t)+\boldsymbol{A}_i(x)\hat{\boldsymbol{y}}(x,t)+\boldsymbol{G}_i(x)\boldsymbol{u}(x,t)\\ &+\boldsymbol{L}_i(x)[\boldsymbol{y}_c(x,t)-\hat{\boldsymbol{y}}_c(x,t)],\quad i\in\mathcal{S}\end{aligned}\tag{9}$$

subject to the boundary condition

$$\boldsymbol{E}_1\hat{\boldsymbol{y}}(z_1,t)+\boldsymbol{E}_2\hat{\boldsymbol{y}}(z_2,t)=\hat{\boldsymbol{d}}(t)$$

and the initial condition

$$\hat{\boldsymbol{y}}(x,0)=\hat{\boldsymbol{y}}_0(x)$$

where $\hat{\boldsymbol{y}}_0(x)$ is the initial state estimate, $\hat{\boldsymbol{d}}(t)$ is the estimated boundary condition, and $\boldsymbol{L}_i(x)$, $i\in\mathcal{S}$ are the $n\times p$ observer gain matrices to be determined, and $\hat{\boldsymbol{y}}_c(x,t)=\boldsymbol{C}(\xi,x)\hat{\boldsymbol{y}}(x,t)$.

The overall fuzzy observer is represented as follows

$$\begin{aligned}\frac{\partial\hat{\boldsymbol{y}}(x,t)}{\partial t}&=\boldsymbol{A}\hat{\boldsymbol{y}}(x,t)+\boldsymbol{A}(\xi,x)\hat{\boldsymbol{y}}(x,t)+\boldsymbol{G}(\xi,x)\boldsymbol{u}(x,t)\\ &+\boldsymbol{L}(\xi,x)[\boldsymbol{y}_c(x,t)-\hat{\boldsymbol{y}}_c(x,t)]\end{aligned}\tag{10}$$

where

$$\boldsymbol{L}(\xi,x)=\sum_{i=1}^{r}h_i(\xi(x,t))\boldsymbol{L}_i(x).$$

In the presence of the fuzzy observer, the PDC-based distributed fuzzy controller takes on the following form:

Control Rule j:
IF $\xi_1(x,t)$ is F_{j1} and … and $\xi_l(x,t)$ is F_{jl}

$$\textbf{THEN}\ \boldsymbol{u}(x,t)=\boldsymbol{K}_j(x)\hat{\boldsymbol{y}}(x,t),\quad j\in\mathcal{S}\tag{11}$$

where $K_j(x)$, $j\in\mathcal{S}$ are the $m\times n$ controller gain matrices to be determined.

The overall fuzzy controller is inferred as follows

$$\boldsymbol{u}(x,t)=\sum_{j=1}^{r}h_j(\xi(x,t))\boldsymbol{K}_j(x)\hat{\boldsymbol{y}}(x,t)=\boldsymbol{K}(\xi,x)\hat{\boldsymbol{y}}(x,t)\tag{12}$$

Remark 1. It is noteworthy that in this study the premise variables $\xi(x,t)$ are required to be available for the construction of fuzzy observer and fuzzy controller. If the premise variables depend on the estimated state variables, that is, $\hat{\xi}(x,t)$ instead of $\xi(x,t)$, the situation becomes more complicated. In this case, it is more difficult to find controller gain matrices $\boldsymbol{K}_j(x)$, $j\in\mathcal{S}$ and observer gain matrices $\boldsymbol{L}_i(x)$,

$i \in \mathcal{S}$. The similar problem is also discussed for T–S fuzzy ODE system.[22]

Remark 2. It must be stressed that this study assumes distributed sensing and actuation. Although this is normally recognized as a critical drawback, with recent advances in technological developments of Micro-Electro-Mechanical Systems, it becomes feasible to manufacture large arrays of microsensors and actuators with integrated control circuitry, which can be used for the implementation of distributed feedback control loops in some practical applications (see Ref. 34 and the references therein). On the other hand, the developed framework of analysis paves the way for further improvements, such as point-wise (or boundary) control and/or sensing, that will be addressed in future research activities. Moreover, different forms of actuator distribution function lead to different control forms[1] (for instance, the actuator distribution function given by the Heaviside step function will yield the piece-wise uniform control form). Therefore, how to obtain more elaborate actuator distributions is also our further research topic.

Define $\boldsymbol{e}(x,t)=\boldsymbol{y}(x,t)-\hat{\boldsymbol{y}}(x,t)$. From Eqs. 6–8, 10, and 12, we have the following augmented closed-loop fuzzy PDE system

$$\frac{\partial \tilde{\boldsymbol{y}}(x,t)}{\partial t}=\tilde{\boldsymbol{A}}\tilde{\boldsymbol{y}}(x,t)+\tilde{\boldsymbol{A}}_c(\xi,x)\tilde{\boldsymbol{y}}(x,t) \tag{13}$$

$$z(x,t)=\tilde{\boldsymbol{H}}_c(\xi,x)\tilde{\boldsymbol{y}}(x,t) \tag{14}$$

subject to the boundary condition

$$\tilde{\boldsymbol{E}}_1\tilde{\boldsymbol{y}}(z_1,t)+\tilde{\boldsymbol{E}}_2\tilde{\boldsymbol{y}}(z_2,t)=\tilde{\boldsymbol{d}}(t)$$

and the initial condition

$$\tilde{\boldsymbol{y}}(x,0)=\tilde{\boldsymbol{y}}_0(x)$$

where $\tilde{\boldsymbol{y}}(x,t)=\begin{bmatrix}\boldsymbol{y}^T(x,t) & \boldsymbol{e}^T(x,t)\end{bmatrix}^T$ and $\tilde{\boldsymbol{y}}_0(x)=\begin{bmatrix}\boldsymbol{y}_0^T(x) & \boldsymbol{e}_0^T(x)\end{bmatrix}^T$, and

$$\tilde{\boldsymbol{A}}_c(\xi,x)=\begin{bmatrix}\boldsymbol{A}(\xi,x)+\boldsymbol{G}(\xi,x)\boldsymbol{K}(\xi,x) & -\boldsymbol{G}(\xi,x)\boldsymbol{K}(\xi,x)\\ 0 & \boldsymbol{A}(\xi,x)-\boldsymbol{L}(\xi,x)\boldsymbol{C}(\xi,x)\end{bmatrix},$$

$$\tilde{\boldsymbol{H}}_c(\xi,x)=[\boldsymbol{H}(\xi,x)+\boldsymbol{D}(\xi,x)\boldsymbol{K}(\xi,x) \quad -\boldsymbol{D}(\xi,x)\boldsymbol{K}(\xi,x)],$$

$\tilde{\boldsymbol{d}}(t)=\begin{bmatrix}\boldsymbol{d}^T(t) & \boldsymbol{d}^T(t)-\hat{\boldsymbol{d}}^T(t)\end{bmatrix}^T$, $\tilde{\boldsymbol{U}}=\mathrm{diag}\{\boldsymbol{U},\boldsymbol{U}\}$ with $\boldsymbol{U}\in\{\boldsymbol{A},\boldsymbol{E}_1,\boldsymbol{E}_2\}$

We consider the following quadratic cost function

$$J=\int_0^\infty \langle \boldsymbol{z}(\cdot,t),\boldsymbol{W}(\cdot)\boldsymbol{z}(\cdot,t)\rangle dt \tag{15}$$

where $\boldsymbol{W}(x)>0$, $x\in[z_1,z_2]$ is a known weighting matrix function.

Hence, the problem considered in this article is to seek a distributed fuzzy observer-based controller of the form in Eqs. 10 and 12 for the PDE system of Eqs. 1 based on the fuzzy PDE model of Eqs. 6 and determine a cost bound $J_b<+\infty$ as small as possible, such that the closed-loop PDE system of Eqs. 13 and 14 is exponentially stable on the Hilbert space $\mathscr{H}^n$, and the cost function defined by Eq. 15 satisfies $J\leq J_b$.

GCDF Observer-Based Control Design

In this section, we aim to develop an SDLMI-based method for the design of a distributed fuzzy observer-based controller such that the resulting closed-loop PDE system is exponentially stable and an optimized upper bound of quadratic cost function is provided. Furthermore, an LMI algorithm is presented to approximately solve the SDLMI optimization problem via the finite difference method.

Based on the fuzzy PDE model of Eqs. 6–8, we have the following result, which provides a GCDF observer-based control design in terms of space-dependent bilinear matrix inequalities (SDBMIs).

Theorem 1. Consider the fuzzy PDE system of Eq. 6 and the cost function in Eq. 15. If there exist a $2n\times 2n$ real matrix $\boldsymbol{P}(x)>0$, $m\times n$ real matrices $\boldsymbol{K}_i(x)$, and $n\times p$ real matrices $\boldsymbol{L}_i(x)$, $i\in\mathcal{S}$ such that the following SDBMIs are satisfied for all $x\in[z_1,z_2]$

$$\tilde{\Theta}_{ii}(x)<0,\quad i\in\mathcal{S}, \tag{16}$$

$$\frac{1}{r-1}\tilde{\Theta}_{ii}(x)+\frac{1}{2}\left(\tilde{\Theta}_{ij}(x)+\tilde{\Theta}_{ji}(x)\right)<0,\quad i\neq j,\quad i,j\in\mathcal{S} \tag{17}$$

where

$$\tilde{\Theta}_{ij}(x)=\begin{bmatrix}\Theta_{ij}(x) & \tilde{\boldsymbol{H}}^T_{c,ij}(x)\\ \tilde{\boldsymbol{H}}_{c,ij}(x) & -\boldsymbol{W}^{-1}(x)\end{bmatrix}<0,\quad i,j\in\mathcal{S},$$

in which

$$\begin{aligned}\Theta_{ij}(x)&=\boldsymbol{P}(x)\tilde{\boldsymbol{A}}_{c,ij}(x)+\tilde{\boldsymbol{A}}^T_{c,ij}(x)\boldsymbol{P}(x)\\&-\frac{d}{dx}(\theta(x)\boldsymbol{P}(x))+[\delta(x-z_2)-\delta(x-z_1)]\theta(x)\boldsymbol{P}(x),\\ \tilde{\boldsymbol{H}}_{c,ij}(x)&=[\boldsymbol{H}_{c,ij}(x) \quad -\boldsymbol{D}_j(x)\boldsymbol{K}_i(x)],\end{aligned}$$

with

$$\tilde{\boldsymbol{A}}_{c,ij}(x)=\begin{bmatrix}\boldsymbol{A}_i(x)+\boldsymbol{G}_j(x)\boldsymbol{K}_i(x) & -\boldsymbol{G}_j(x)\boldsymbol{K}_i(x)\\ 0 & \boldsymbol{A}_i(x)-\boldsymbol{L}_i(x)\boldsymbol{C}_j(x)\end{bmatrix},$$

then there exists a fuzzy observer-based controller of the form in Eqs. 10 and 12 such that the closed-loop PDE system of Eqs. 13 and 14 is exponentially stable, and the cost function in Eq. 15 satisfies

$$J<J_b=\langle\tilde{\boldsymbol{y}}_0(\cdot),\boldsymbol{P}(\cdot)\tilde{\boldsymbol{y}}_0(\cdot)\rangle. \tag{18}$$

Proof. See Appendix A

Remark 3. From a purely mathematical viewpoint, the Dirac delta function used in the SDBMIs in Eqs. 16 and 17 is not strictly a function, because any extended-real function that is equal to zero everywhere but a single point must have total integral zero. While for many purpose this function can be manipulated as a function, formally it can be defined as a distribution function that is also a measure. Furthermore, one may use the following approximation to the Dirac delta function[35,36]

$$\delta(x-x_b)\approx\begin{cases}\eta^{-1} & \text{if } x\in[x_b-\eta/2,x_b+\eta/2]\\ 0 & \text{otherwise}\end{cases}.$$

Theorem 1 provides not only a sufficient condition for the solvability of GCDF observer-based control design problem for the fuzzy PDE system of Eqs. 6–8 but also an upper bound $J_b=\langle\tilde{\boldsymbol{y}}_0(\cdot),\boldsymbol{P}(\cdot)\tilde{\boldsymbol{y}}_0(\cdot)\rangle$ for the cost function in Eq. 15. On the other hand, it is easily observed that the inequalities in Eqs. 16 and 17 are SDBMIs with respect to the decision variables in the set $\{\boldsymbol{P}(x),\boldsymbol{K}_i(x),\boldsymbol{L}_i(x),i\in\mathcal{S}\}$, which are BMIs in nature. In contrast to LMI problems, which are convex and can be solved approximately by the polynomial-time interior-point method,[32,33] BMI problems are nonconvex and known to be NP-hard.[37] Hence, the SDBMIs in Eqs. 16 and 17 are still inefficient to solve by the present solvers.

In the following theorem, we will present an approach to transform equivalently the SDBMIs in Eqs. 16 and 17 into SDLMIs so as to determine the feedback control gains $\boldsymbol{K}_i(x)$ and the observer gains $\boldsymbol{L}_i(x)$. To this end, we set $\hat{\boldsymbol{y}}_0(x)=\boldsymbol{y}_0(x)$, that is, $\tilde{\boldsymbol{y}}_0(x)=\begin{bmatrix}\boldsymbol{y}_0^T(x) & 0\end{bmatrix}^T$.

Theorem 2. The SDBMIs in Eqs. 16 and 17 have feasible solutions $\boldsymbol{P}(x)>0$, $\boldsymbol{K}_i(x)$, and $\boldsymbol{L}_i(x)$, $i \in \mathcal{S}$, if and only if the following SDLMIs have feasible solutions $\boldsymbol{Q}_1(x)>0$, $\boldsymbol{Q}_2(x)>0$, $\boldsymbol{N}_i(x)$, $\boldsymbol{Z}_i(x)$, $i \in \mathcal{S}$:

$$\tilde{\Phi}_{1,ii}(x) < 0, \quad i \in \mathcal{S} \tag{19}$$

$$\frac{1}{r-1}\tilde{\Phi}_{1,ii}(x)+\frac{1}{2}\left(\tilde{\Phi}_{1,ij}(x)+\tilde{\Phi}_{1,ji}(x)\right) < 0, \quad i \neq j, \quad i,j \in \mathcal{S} \tag{20}$$

$$\tilde{\Phi}_{2,ii}(x) < 0, \quad i \in \mathcal{S} \tag{21}$$

$$\frac{1}{r-1}\tilde{\Phi}_{2,ii}(x)+\frac{1}{2}\left(\tilde{\Phi}_{2,ij}(x)+\tilde{\Phi}_{2,ji}(x)\right) < 0, \quad i \neq j, \quad i,j \in \mathcal{S} \tag{22}$$

where

$$\tilde{\Phi}_{1,ij}(x)=\begin{bmatrix}\theta(x)d\boldsymbol{Q}_1(x)/dx+\tilde{\Psi}_{11,ij}(x) & \tilde{\Psi}_{12,ij}(x) \\ \tilde{\Psi}^T_{12,ij}(x) & -\boldsymbol{W}^{-1}(x)\end{bmatrix}, \quad i,j \in \mathcal{S},$$

$$\tilde{\Phi}_{2,ij}(x)=-\theta(x)d\boldsymbol{Q}_2(x)/dx+\tilde{\Psi}_{2,ij}(x), \quad i,j \in \mathcal{S},$$

with

$$\tilde{\Psi}_{11,ij}(x)=\boldsymbol{A}_i(x)\boldsymbol{Q}_1(x)+\boldsymbol{Q}_1(x)\boldsymbol{A}_i^T(x)+\boldsymbol{G}_j(x)\boldsymbol{N}_i(x)+\boldsymbol{N}_i^T(x)\boldsymbol{G}_j^T(x)-d\theta(x)/dx\boldsymbol{Q}_1(x)+[\delta(x-z_2)-\delta(x-z_1)]\theta(x)\boldsymbol{Q}_1(x),$$

$$\tilde{\Psi}_{12,ij}(x)=\boldsymbol{Q}_1(x)\boldsymbol{H}_i^T(x)+\boldsymbol{N}_i^T(x)\boldsymbol{D}_j^T(x),$$

$$\tilde{\Psi}_{2,ij}(x)=-d\theta(x)/dx\boldsymbol{Q}_2(x)+\boldsymbol{Q}_2(x)\boldsymbol{A}_i(x)+\boldsymbol{A}_i^T(x)\boldsymbol{Q}_2(x)-\boldsymbol{Z}_i(x)\boldsymbol{C}_j(x)-\boldsymbol{C}_j^T(x)\boldsymbol{Z}_i^T(x)+[\delta(x-z_2)-\delta(x-z_1)]\theta(x)\boldsymbol{Q}_2(x).$$

In this case, the cost function in Eq. 15 satisfies

$$J < J_b=\langle \boldsymbol{y}_0(\cdot), \boldsymbol{Q}_1^{-1}(\cdot)\boldsymbol{y}_0(\cdot)\rangle \tag{23}$$

and the control gain matrices $\boldsymbol{K}_i(x)$ and the observer gain matrices $\boldsymbol{L}_i(x)$, $i \in \mathcal{S}$ are given by

$$\boldsymbol{K}_i(x)=\boldsymbol{N}_i(x)\boldsymbol{Q}_1^{-1}(x), \quad \boldsymbol{L}_i(x)=\boldsymbol{Q}_2^{-1}(x)\boldsymbol{Z}_i(x), \quad i \in \mathcal{S} \tag{24}$$

Proof. See Appendix B.

To make the upper bound J_b of J in Eq. 23 as small as possible, we seek to minimize the following upper bound of J_b:

$$J_b=\langle \boldsymbol{y}_0(\cdot), \boldsymbol{Q}_1^{-1}(\cdot)\boldsymbol{y}_0(\cdot)\rangle < \rho. \tag{25}$$

By Schur complement,[32] it is easy to verify that the inequality in Eq. 25 holds if the following SDLMI holds

$$\begin{bmatrix}\rho(z_2-z_1)^{-1} & \boldsymbol{y}_0^T(x) \\ \boldsymbol{y}_0(x) & \boldsymbol{Q}_1(x)\end{bmatrix} > 0. \tag{26}$$

Therefore, a suboptimal control design can be formulated as the following SDLMI optimization problem:

$$\min_{\mathcal{U}} \rho \text{ subject to the SDLMIs in Eqs .19–22 and 26} \tag{27}$$

where

$$\mathcal{U}=\{\rho, \boldsymbol{Q}_1(x), \boldsymbol{Q}_2(x), \boldsymbol{N}_i(x), \boldsymbol{Z}_i(x), i \in \mathcal{S}\}. \tag{27}$$

As its space-distributed characteristic, the optimization problem in Eq. 27 cannot be directly solved by using the standard LMI optimization techniques. In what follows, we will develop an algorithm to approximately solve the SDLMI optimization problem in Eq. 27. To this end, let us discretize the space interval $[z_1, z_2]$ into space instances $\{x_k, k \in \mathcal{N}, x_0=z_1, x_N=z_2\}$ of the same distance, where

$$x_k-x_{k-1}=\varepsilon=(z_2-z_1)/N, \quad \mathcal{N}=\{0,1,\cdots,N\} \tag{28}$$

and use the backward difference for the spatial derivative, that is,

$$\frac{d\boldsymbol{O}(x)}{dx} \approx \frac{\boldsymbol{O}(x_k)-\boldsymbol{O}(x_{k-1})}{\varepsilon} \tag{29}$$

where $\boldsymbol{O}(x)$ stands for the space-varying matrix function with appropriated dimensions.

Using Eq. 29, the SDLMIs in Eqs. 19–22 and 26 can be approximated by the following LMIs with respect to $\boldsymbol{Q}_1(x_{-1})>0$, $\boldsymbol{Q}_1(x_k)>0$, $\boldsymbol{Q}_2(x_{-1})>0$, $\boldsymbol{Q}_2(x_k)>0$, $\boldsymbol{N}_i(x_k)$, and $\boldsymbol{Z}_i(x_k)$, $i \in \mathcal{S}$, $k \in \mathcal{N}$:

$$\hat{\Phi}_{1,ii}(x_k) < 0, \quad k \in \mathcal{N}, \quad i \in \mathcal{S} \tag{30}$$

$$\frac{1}{r-1}\hat{\Phi}_{1,ii}(x_k)+\frac{1}{2}\left(\hat{\Phi}_{1,ij}(x_k)+\hat{\Phi}_{1,ji}(x_k)\right) < 0, \quad k \in \mathcal{N}, \quad i \neq j, \quad i,j \in \mathcal{S} \tag{31}$$

$$\hat{\Phi}_{2,ii}(x_k) < 0, \quad k \in \mathcal{N}, \quad i \in \mathcal{S} \tag{32}$$

$$\frac{1}{r-1}\hat{\Phi}_{2,ii}(x_k)+\frac{1}{2}\left(\hat{\Phi}_{2,ij}(x_k)+\hat{\Phi}_{2,ji}(x_k)\right) < 0, \quad k \in \mathcal{N}, \quad i \neq j, \quad i,j \in \mathcal{S}, \tag{33}$$

$$\begin{bmatrix}\rho(z_2-z_1)^{-1} & \boldsymbol{y}_0^T(x_k) \\ \boldsymbol{y}_0(x_k) & \boldsymbol{Q}_1(x_k)\end{bmatrix} > 0, \quad k \in \mathcal{N} \tag{34}$$

where

$$\hat{\Phi}_{1,ij}(x_k)=\begin{bmatrix}\theta(x_k)\dfrac{\boldsymbol{Q}_1(x_k)-\boldsymbol{Q}_1(x_{k-1})}{\varepsilon}+\tilde{\Psi}_{11,ij}(x_k) & \tilde{\Psi}_{12,ij}(x_k) \\ \tilde{\Psi}^T_{12,ij}(x_k) & -\boldsymbol{W}^{-1}(x_k)\end{bmatrix}, \quad i,j \in \mathcal{S},$$

$$\hat{\Phi}_{2,ij}(x_k)=-\theta(x_k)\frac{\boldsymbol{Q}_2(x_k)-\boldsymbol{Q}_2(x_{k-1})}{\varepsilon}+\tilde{\Psi}_{2,ij}(x_k), \quad i,j \in \mathcal{S},$$

in which the definitions on $\tilde{\Psi}_{11,ij}(\cdot)$, $\tilde{\Psi}_{12,ij}(\cdot)$, and $\tilde{\Psi}_{2,ij}(\cdot)$, $i,j \in \mathcal{S}$ are given in Theorem 2.

Table 1. Model Parameters Used in Numerical Simulations

Process Parameters	Numerical Values
υ	0.025 m/s
L	1 m
E	12,000 cal/mol
k_0	10^6 s^{-1}
b	0.4 s^{-1}
$C_{A,\text{in}}$	1 mol/L
R	1.986 cal/(mol K)
T_{in}	350 K
φ	0.45

Therefore, the suboptimal control design can be formulated as the following approximate LMI optimization problem under a suitable positive integer N

$$\min_{\mathcal{U}} \rho \text{ subject to the LMIs in Eqs. 30–34} \tag{35}$$

where

$$\mathcal{U}=\{\rho, \boldsymbol{Q}_1(x_{-1}), \boldsymbol{Q}_2(x_{-1}), \boldsymbol{Q}_1(x_k), \boldsymbol{Q}_2(x_k), \boldsymbol{N}_i(x_k), \boldsymbol{Z}_i(x_k), i \in \mathcal{S}, k \in \mathcal{N}\},$$

which can be solved efficiently using the standard LMI optimization techniques. If the optimal solution ρ^* is found, using the solutions $\boldsymbol{Q}_1(x_k)$, $\boldsymbol{Q}_2(x_k)$, $\boldsymbol{N}_i(x_k)$, and $\boldsymbol{Z}_i(x_k)$, $i \in \mathcal{S}$, $k \in \mathcal{N}$ of the problem in Eq. 35, the actual upper bound of J can be given by $J_b \approx \varepsilon \sum_{k=0}^{N} \boldsymbol{y}_0^T(x_k)\boldsymbol{Q}_1^{-1}(x_k)\boldsymbol{y}_0(x_k)$ and the corresponding control gain matrices and the observer gain matrices are obtained by

$$\boldsymbol{K}_i(x_k)=\boldsymbol{N}_i(x_k)\boldsymbol{Q}_1^{-1}(x_k), \quad \boldsymbol{L}_i(x_k)=\boldsymbol{Q}_2^{-1}(x_k)\boldsymbol{Z}_i(x_k), \quad i \in \mathcal{S}, \quad k \in \mathcal{N}.$$

It is noteworthy that based on the finite difference theory,[38] the accuracy of difference approximation in Eq. 29 depends on the chosen value of positive integer N and the approximation error of Eq. 29 converges to zero when $N \to \infty$. If a sufficiently large N is chosen, the SDLMIs in Eqs. 19–22 and 26 will be well approximated by the LMIs in Eqs. 30–34. However, the value of parameter N and the computational cost are generally mutual restraint, that is, the computational cost of the present solver used to solve the problem in Eq. 35 is higher with the increasing of the value of N. Although there exists no exact way to determine *a priori* the size of the spatial discretization step when solving the SDLMI optimization problem, a practical approach is to take the spatial discretization interval to be the smallest possible, which still complies with the computational resources and with the accuracy of the LMI solver used.

Remark 4. Notice that an LMI algorithm[31] has been recently developed to approximately solve the SDLMI feasibility problem. The obvious difference between the algorithm[31] and the algorithm proposed in this study is that the former is a recursive algorithm, which requires giving an initial value $\boldsymbol{Q}(x_{-1})>0$ in advance, whereas the latter is a standard LMI algorithm, where matrices $\boldsymbol{Q}_1(x_{-1})$ and $\boldsymbol{Q}_2(x_{-1})$ are the decision variables of the LMI optimization problem in Eq. 35. Another important difference is that the algorithm[31] is used for solving the SDLMI feasibility problem, whereas the one in this study is developed to solve the SDLMI optimization problem in Eq. 27.

Simulation Example

As a case study, for the purpose of demonstrating the effectiveness of the main theoretical results derived in previous sections, we consider a nonisothermal PFR with the following elementary chemical reaction[2]: $A \to B$.

Process description

The reaction on endothermic and a jacket is used to heat the reactor. Under the assumptions of perfect radial mixing, constant density and heat capacity of the reacting liquid and negligible diffusive phenomena, a dynamic model of the process can be derived from material and energy balances and has the form[31]:

$$\frac{\partial T}{\partial t}=-\upsilon\frac{\partial T}{\partial x}+\frac{(-\Delta H)k_0}{\rho_p C_p}C_A \exp\left(-\frac{E}{RT}\right)+\frac{4h}{\rho_p C_p d}(T_w-T) \tag{36}$$

$$\frac{\partial C_A}{\partial t}=-\upsilon\frac{\partial C_A}{\partial x}-k_0 C_A \exp\left(-\frac{E}{RT}\right) \tag{37}$$

subject to the boundary conditions

$$T(0,t)=T_{\text{in}}, \quad C_A(0,t)=C_{A,\text{in}}$$

and initial conditions

$$T(x,0)=T_0(x), \quad C_A(x,0)=C_{A0}(x)$$

where C_A and T denote the reactant concentration and the temperature in the reactor, respectively, ρ_p and C_P stand for the density and specific heat capacity, respectively, υ denotes the velocity of the fluid phase, h and d denote the wall heat-transfer coefficient and the reactor diameter, respectively, T_w denotes the temperature in the jacket, k_0, E, ΔH denote the pre-exponential factor, the activation energy, and the enthalpy of the reaction, $C_{A,\text{in}}$ and T_{in} denote the concentration and temperature of the inlet stream, $C_{A0}(x)$ and $T_0(x)$ denote the initial concentration and temperature profiles, respectively, such that $T_0(0)=T_{\text{in}}$ and $C_{A0}(0)=C_{A,\text{in}}$. In addition, t, x, and L denote the independent time and space variables, and the length of the PFR, respectively.

To compensate for the large differences in the order of magnitude of the model variables (possibly resulting in numerical simulation inaccuracies), the following dimensionless state variables χ_1 and χ_2 and dimensionless control input χ_w are introduced

$$\chi_1=\frac{T-T_{\text{in}}}{T_{\text{in}}}, \quad \chi_2=\frac{C_{A,\text{in}}-C_A}{C_{A,\text{in}}}, \quad \text{and} \quad \chi_w=\frac{T_w-T_{\text{in}}}{T_{\text{in}}}$$

Then, the model of Eqs. 36 and 37 is rewritten as follows:

$$\frac{\partial \chi_1(x,t)}{\partial t}=-\upsilon\frac{\partial \chi_1(x,t)}{\partial x}+\beta_1(1-\chi_2)\exp\left(\frac{\mu\chi_1}{1+\chi_1}\right)+b(\chi_w-\chi_1) \tag{38}$$

$$\frac{\partial \chi_2(x,t)}{\partial t}=-\upsilon\frac{\partial \chi_2(x,t)}{\partial x}+\beta_2(1-\chi_2)\exp\left(\frac{\mu\chi_1}{1+\chi_1}\right) \tag{39}$$

subject to the boundary conditions:

$$\chi_1(0,t)=0, \quad \chi_2(0,t)=0 \tag{40}$$

and initial conditions:

$$\chi_1(x,0)=\chi_{10}(x), \quad \chi_2(x,0)=\chi_{20}(x)$$

where $\chi_{10}(x)=\frac{T_0(x)-T_{\text{in}}}{T_{\text{in}}}$, $\chi_{20}(x)=\frac{C_{A,\text{in}}-C_{A0}(x)}{C_{A,\text{in}}}$, and the parameters β_1, β_2, φ, b, and μ are defined as follows:

$$\mu = \frac{E}{RT_{\text{in}}}, \quad \beta_1 = \varphi\beta_2, \quad \beta_2 = k_0 \exp(-\mu),$$
$$\varphi = \frac{(-\Delta H)C_{A,\text{in}}}{\rho_p C_p T_{\text{in}}}, b = \frac{4h}{\rho_p C_p d}$$

The equilibrium profiles for the model in Eqs. 38–40 are assumed to be of the form $\chi(x) = [\chi_{1e}(x) \quad \chi_{2e}(x) \quad \chi_{we}(x)]^T$ which satisfy the equations

$$\frac{d\chi_{1e}(x)}{dx} = \frac{\beta_1}{\upsilon}(1-\chi_{2e}(x))\exp\left(\frac{\mu\chi_{1e}(x)}{1+\chi_{1e}(x)}\right) + \frac{b}{\upsilon}(\chi_{we}(x)-\chi_{1e}(x)) \tag{41}$$

$$\frac{d\chi_{2e}(x)}{dx} = \frac{\beta_2}{\upsilon}(1-\chi_{2e}(x))\exp\left(\frac{\mu\chi_{1e}(x)}{1+\chi_{1e}(x)}\right) \tag{42}$$

subject to $\chi_{1e}(0)=0$ and $\chi_{2e}(0)=0$ (43)

In contrast to the result,[31] in this example, we assume that $\chi_{we}(x)=0$. Under this assumption, the equilibrium profiles $[\chi_{1e}(x) \quad \chi_{2e}(x)]^T$ for the model in Eqs. 38–40 can be obtained by solving Eqs. 41–43. Let us consider the new input vector $u(x,t) = \chi_w(x,t) - \chi_{we}(x)$ and the following state transformation

$$\boldsymbol{y}(x,t) = [y_1(x,t) \quad y_2(x,t)]^T = [\chi_1(x,t)-\chi_{1e}(x) \quad \chi_2(x,t)-\chi_{2e}(x)].^T$$

Then, the system of Eqs. 38–40 can be represented as the form of Eqs. 1 and 4 with $\theta(x) = -\upsilon$, $\boldsymbol{G}(\boldsymbol{y}(x,t),x) = \boldsymbol{G}(x) = [b \ 0]^T$, $z_1=0$, $z_2=L=1$

$$\boldsymbol{f}(\boldsymbol{y}(x,t),x) = \begin{bmatrix} \beta_1 f_0(\boldsymbol{y}(x,t),x) - by_1(x,t) \\ \beta_2 f_0(\boldsymbol{y}(x,t),x) \end{bmatrix},$$
$$\boldsymbol{E}_1 = \text{diag}\{1,1\}, \ \boldsymbol{E}_2 = 0, \ \boldsymbol{d}(t) = 0.$$

$$f_0(\boldsymbol{y}(x,t),x) = (1-\chi_{2e}(x))\left[\exp\left(\frac{\mu(y_1(x,t)+\chi_{1e}(x))}{1+y_1(x,t)+\chi_{1e}(x)}\right) - \exp\left(\frac{\mu(\chi_{1e}(x))}{1+\chi_{1e}(x)}\right)\right] - y_2(x,t)\exp\left(\frac{\mu(y_1(x,t)+\chi_{1e}(x))}{1+y_1(x)+\chi_{1e}(x)}\right). \tag{44}$$

The model parameter values are given in Table 1. Using these values, Figure 1 shows the steady-state profiles of temperature and reactant concentration.

The distributed sensing of temperature in the reactor is more feasible than that of the reactant concentration because of the recent advance in the development of the microtemperature sensor technology. Hence, the measured output and controlled output are respectively defined as follows

$$y_c(x,t) = y_1(x,t), \tag{45}$$
$$z(x,t) = y_1(x,t) + u(x,t). \tag{46}$$

Hence, the system of Eqs. 45 and 46 can be represented as the form of Eqs. 2 and 3 with

$$\boldsymbol{h}_c(\boldsymbol{y}(x,t),x) = y_1(x,t), \quad \boldsymbol{h}_z(\boldsymbol{y}(x,t),x) = y_1(x,t), \quad \text{and} \quad \boldsymbol{D}(\boldsymbol{y}(x,t),x) = 1 \tag{47}$$

T–S fuzzy PDE modeling

Let

$\xi_1(y_1(x,t),x) = \exp\left(\frac{\mu(y_1(x,t)+\chi_{1e}(x))}{1+y_1(x,t)+\chi_{1e}}\right) - \exp\left(\frac{\mu\chi_{1e}(x)}{1+\chi_{1e}(x)}\right)$, $\xi_2(y_1(x,t),x) = \exp\left(\frac{\mu(y_1(x,t)+\chi_{1e}(x))}{1+y_1(x,t)+\chi_{1e}(x)}\right)$, where $y_1(x,t) \in [\chi_{1e}(x)-\alpha, \chi_{1e}(x)+\alpha]$ and α is a given positive value. Then, the nonlinear term $\boldsymbol{f}(\boldsymbol{y}(x,t),x)$ in Eq. 44 can be rewritten as

$$\boldsymbol{f}(\boldsymbol{y}(x,t),x) = \begin{bmatrix} \beta_1\{(1-\chi_{2e}(x))\xi_1(y_1(x,t),x) - \xi_2(y_1(x,t),x)y_2(x,t)\} - by_1(x,t) \\ \beta_2\{(1-\chi_{2e}(x))\xi_1(y_1(x,t),x) - \xi_2(y_1(x,t),x)y_2(x,t)\} \end{bmatrix}.$$

By considering $y_1(x,t) \in [\chi_{1e}(x)-\alpha, \chi_{1e}(x)+\alpha]$ and the fact that $\xi_1(y_1(x,t),x)$ and $\xi_2(y_1(x,t),x)$ are monotonically increasing functions with respect to $y_1(x,t)$, we have

$$\xi_1(y_1(x,t),x) \in \left[\theta_1(x) - \exp\left(\frac{\mu\chi_{1e}(x)}{1+\chi_{1e}(x)}\right), \theta_2(x) - \exp\left(\frac{\mu\chi_{1e}(x)}{1+\chi_{1e}(x)}\right)\right],$$

$\xi_2(y_1(x,t),x) \in [\theta_1(x), \theta_2(x)]$, $\theta_1(x) = \exp\left(\frac{\mu(-\alpha+2\chi_{1e}(x))}{1-\alpha+2\chi_{1e}(x)}\right)$, $\theta_2(x) = \exp\left(\frac{\mu(\alpha+2\chi_{1e}(x))}{1+\alpha+2\chi_{1e}(x)}\right)$.

Thus, the terms $\xi_1(y_1(x,t),x)$ and $\xi_2(y_1(x,t),x)$ can be represented as

$$\begin{aligned} &\xi_1(y_1(x,t),x) = F_{11}(\xi_1(y_1(x,t),x))\kappa_1(x)y_1(x,t) + \\ &F_{21}(\xi_1(y_1(x,t),x))\kappa_2(x)y_1(x,t), \\ &\xi_2(y_1(x,t),x) = F_{12}(\xi_2(y_1(x,t),x))\theta_1(x) + F_{22}(\xi_2(y_1(x,t),x))\theta_2(x) \end{aligned} \tag{48}$$

where $\kappa_1(x) = -\alpha^{-1}\left(\theta_1(x) - \exp\left(\frac{\mu\chi_{1e}(x)}{1+\chi_{1e}(x)}\right)\right)$, $\kappa_2(x) = \alpha^{-1}\left(\theta_2(x) - \exp\left(\frac{\mu\chi_{1e}(x)}{1+\chi_{1e}(x)}\right)\right)$, $F_{11}(\xi_1(y_1(x,t),x))$, $F_{21}(\xi_1(y_1(x,t),x))$, $F_{12}(\xi_2(y_1(x,t),x))$. $F_{22}(\xi_2(y_1(x,t),x)) \in [0,1]$, and

$$\begin{aligned} &F_{11}(\xi_1(y_1(x,t),x)) + F_{21}(\xi_1(y_1(x,t),x)) = 1, \\ &F_{12}(\xi_2(y_1(x,t),x)) + F_{22}(\xi_2(y_1(x,t),x)) = 1. \end{aligned} \tag{49}$$

Solving Eqs. 48 and 49 gives

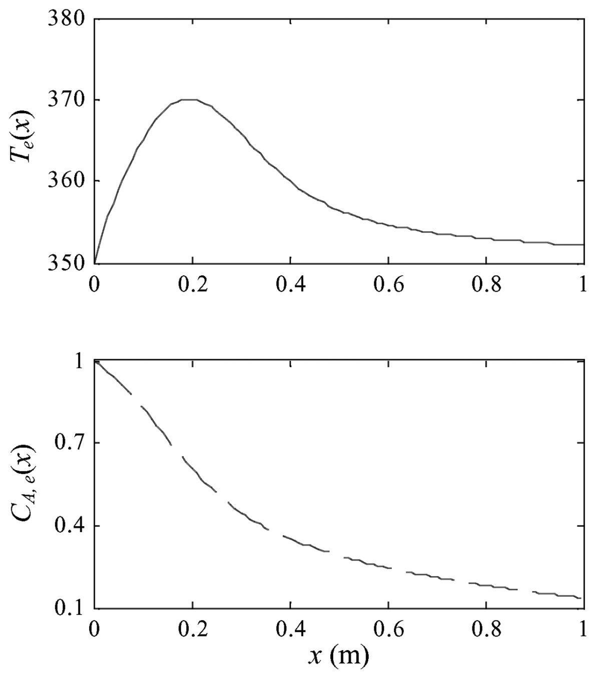

Figure 1. Steady-state profiles of temperature and reactant concentration.

$$F_{11}(\xi_1(y_1(x,t),x))=\begin{cases}\dfrac{\xi_1(y_1(x,t),x)-\kappa_2(x)y_1(x,t)}{y_1(x,t)(\kappa_1(x)-\kappa_2(x))}, & y_1(x,t)\neq 0\\ (\varpi-\kappa_2(x))/(\kappa_1(x)-\kappa_2(x)), & y_1(x,t)=0,\end{cases}$$

$$F_{21}(\xi_1(y_1(x,t),x))=1-F_{11}(\xi_1(y_1(x,t),x)),$$
$$F_{12}(\xi_2(y_1(x,t),x))=\frac{\theta_2(x)-\xi_2(y_1(x,t),x)}{\theta_2(x)-\theta_1(x)},$$
$$F_{22}(\xi_2(y_1(x,t),x))=1-F_{12}(\xi_2(y_1(x,t),x)),$$

where $$\varpi=\lim_{y_1(x,t)\to 0}\xi_1(y_1(x,t),x)/y_1(x,t).$$

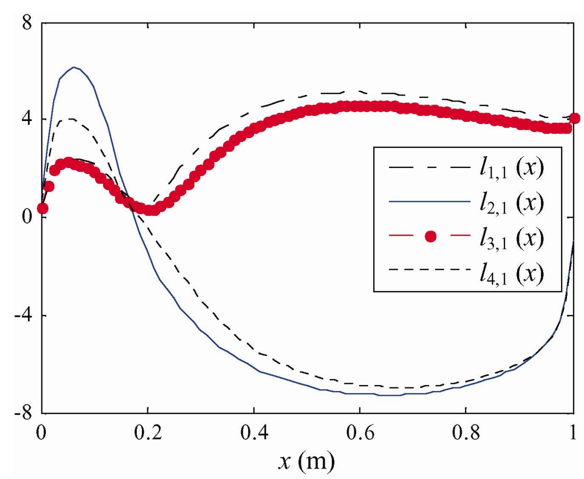

Figure 2. The observer gain matrices $l_{i,1}(x)$, $i\in\{1,2,3,4\}$.

[Color figure can be viewed in the online issue, which is available at wileyonlinelibrary.com.]

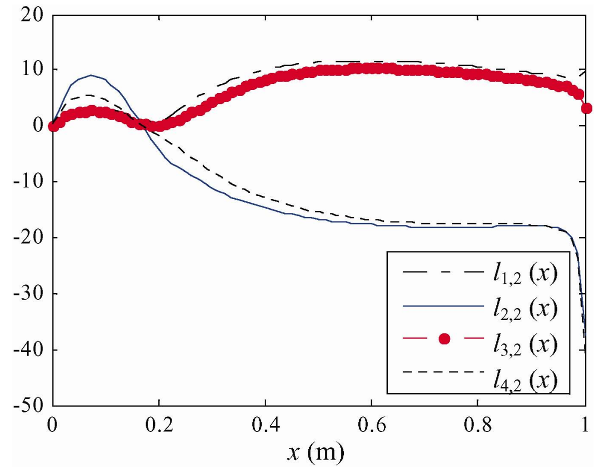

Figure 3. The observer gain matrices $l_{i,2}(x)$, $i\in\{1,2,3,4\}$.

[Color figure can be viewed in the online issue, which is available at wileyonlinelibrary.com.]

From above analysis, hence, the PDE system of Eqs. 1–3 with Eqs. 44 and 47 can be represented by the following T–S fuzzy PDE model of four rules:

Plant Rule 1:

IF $\xi_1(y_1(x,t),x)$ is about $\theta_1(x)-\exp\left(\frac{\mu\chi_{1e}(x)}{1+\chi_{1e}(x)}\right)$ and $\xi_2(y_1(x,t),x)$ is about $\theta_1(x)$,

$$\textbf{THEN}\begin{cases}\partial\boldsymbol{y}(x,t)/\partial t=\boldsymbol{A}\boldsymbol{y}(x,t)+\boldsymbol{A}_1(x)\boldsymbol{y}(x,t)+\boldsymbol{G}_1(x)u(x,t)\\ y_c(x,t)=\boldsymbol{C}_1(x)\boldsymbol{y}(x,t)\\ z(x,t)=\boldsymbol{H}_1(x)\boldsymbol{y}(x,t)+\boldsymbol{D}_1(x)u(x,t)\end{cases}$$

Plant Rule 2:

IF $\xi_1(y_1(x,t),x)$is about $\theta_2(x)-\exp\left(\frac{\mu\chi_{1e}(x)}{1+\chi_{1e}(x)}\right)$ and $\xi_2(y_1(x,t),x)$ is about $\theta_1(x)$

$$\textbf{THEN}\begin{cases}\partial\boldsymbol{y}(x,t)/\partial t=\boldsymbol{A}\boldsymbol{y}(x,t)+\boldsymbol{A}_2(x)\boldsymbol{y}(x,t)+\boldsymbol{G}_2(x)u(x,t)\\ y_c(x,t)=\boldsymbol{C}_2(x)\boldsymbol{y}(x,t)\\ z(x,t)=\boldsymbol{H}_2(x)\boldsymbol{y}(x,t)+\boldsymbol{D}_2(x)u(x,t)\end{cases}$$

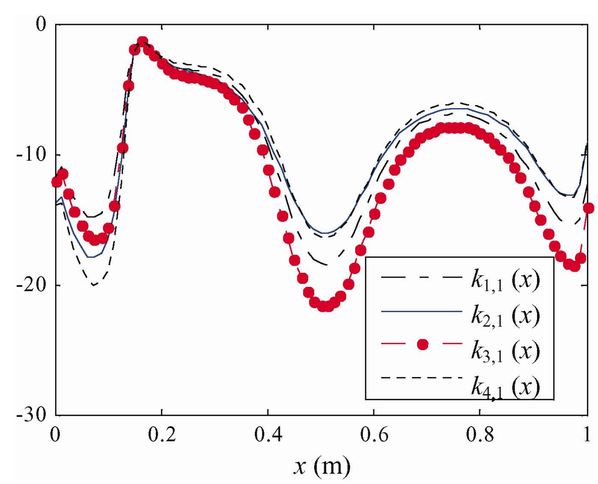

Figure 4. The control gain matrices $k_{i,1}(x)$, $i\in\{1,2,3,4\}$.

[Color figure can be viewed in the online issue, which is available at wileyonlinelibrary.com.]

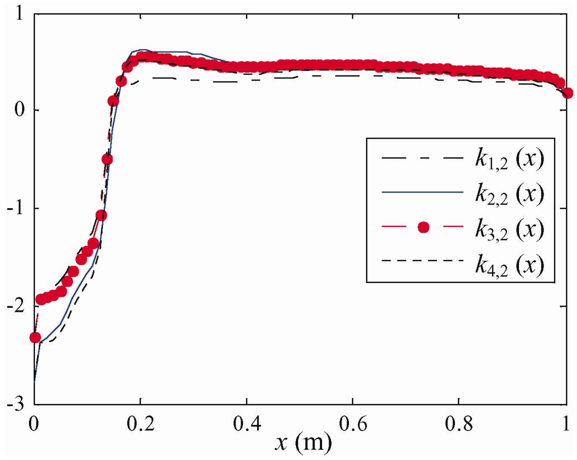

Figure 5. The control gain matrices $k_{i,2}(x)$, $i\in\{1,2,3,4\}$.

[Color figure can be viewed in the online issue, which is available at wileyonlinelibrary.com.]

Plant Rule 3:

IF $\xi_1(y_1(x,t),x)$ is about $\theta_1(x)-\exp\left(\frac{\mu\chi_{1e}(x)}{1+\chi_{1e}(x)}\right)$ and $\xi_2(y_1(x,t),x)$ is about $\theta_2(x)$

$$\textbf{THEN}\begin{cases}\partial\boldsymbol{y}(x,t)/\partial t=\boldsymbol{A}\boldsymbol{y}(x,t)+\boldsymbol{A}_3(x)\boldsymbol{y}(x,t)+\boldsymbol{G}_3(x)u(x,t)\\ y_c(x,t)=\boldsymbol{C}_3(x)\boldsymbol{y}(x,t)\\ z(x,t)=\boldsymbol{H}_3(x)\boldsymbol{y}(x,t)+\boldsymbol{D}_3(x)u(x,t)\end{cases}$$

Plant Rule 4:

IF $\xi_1(y_1(x,t),x)$ is about $\theta_2(x)-\exp\left(\frac{\mu\chi_{1e}(x)}{1+\chi_{1e}(x)}\right)$ and $\xi_2(y_1(x,t),x)$ is about $\theta_2(x)$

$$\textbf{THEN}\begin{cases}\partial\boldsymbol{y}(x,t)/\partial t=\boldsymbol{A}\boldsymbol{y}(x,t)+\boldsymbol{A}_4(x)\boldsymbol{y}(x,t)+\boldsymbol{G}_4(x)u(x,t)\\ y_c(x,t)=\boldsymbol{C}_4(x)\boldsymbol{y}(x,t)\\ z(x,t)=\boldsymbol{H}_4(x)\boldsymbol{y}(x,t)+\boldsymbol{D}_4(x)u(x,t)\end{cases}$$

where

$$\boldsymbol{A}_1(x)=\begin{bmatrix}\beta_1(1-\chi_{2e}(x))\kappa_1(x)-b & -\beta_1\theta_1(x)\\ \beta_2(1-\chi_{2e}(x))\kappa_1(x) & -\beta_2\theta_1(x)\end{bmatrix},$$

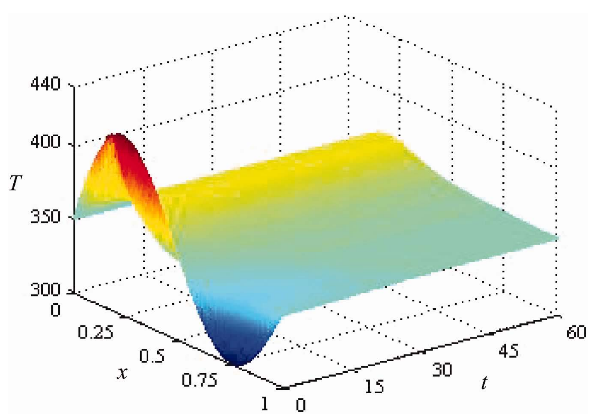

Figure 6. Closed-loop profile of evolution of temperature.

[Color figure can be viewed in the online issue, which is available at wileyonlinelibrary.com.]

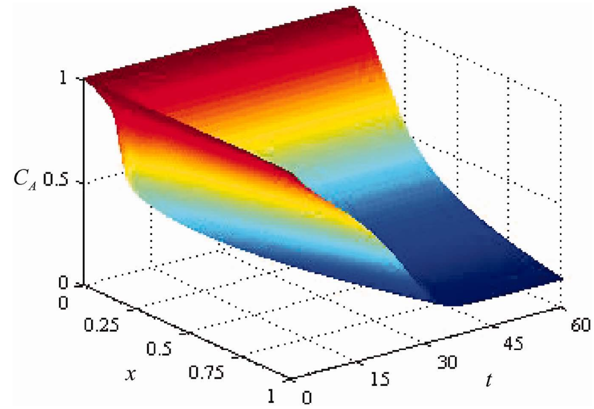

Figure 7. Closed-loop profile of evolution of reactant concentration.

[Color figure can be viewed in the online issue, which is available at wileyonlinelibrary.com.]

$$\boldsymbol{A}_2(x)=\begin{bmatrix}\beta_1(1-\chi_{2e}(x))\kappa_2(x)-b & -\beta_1\theta_1(x)\\ \beta_2(1-\chi_{2e}(x))\kappa_2(x) & -\beta_2\theta_1(x)\end{bmatrix},$$

$$\boldsymbol{A}_3(x)=\begin{bmatrix}\beta_1(1-\chi_{2e}(x))\kappa_1(x)-b & -\beta_1\theta_2(x)\\ \beta_2(1-\chi_{2e}(x))\kappa_1(x) & -\beta_2\theta_2(x)\end{bmatrix},$$

$$\boldsymbol{A}_4(x)=\begin{bmatrix}\beta_1(1-\chi_{2e}(x))\kappa_2(x)-b & -\beta_1\theta_2(x)\\ \beta_2(1-\chi_{2e}(x))\kappa_2(x) & -\beta_2\theta_2(x)\end{bmatrix},$$

$$\boldsymbol{G}_i(x)=\boldsymbol{G}(x)=[b\ 0]^T,\boldsymbol{C}_i(x)=\boldsymbol{C}(x)=[1\ 0],\boldsymbol{H}_i(x)=\boldsymbol{H}(x)=[1\ 0],\boldsymbol{D}_i(x)=\boldsymbol{D}(x)=1,i\in\{1,2,3,4\}.$$

Thus, the overall fuzzy PDE model is given by

$$\frac{\partial\boldsymbol{y}(x,t)}{\partial t}=\boldsymbol{A}\boldsymbol{y}(x,t)+\sum_{i=1}^{4}h_i(\xi)\boldsymbol{A}_i(x)\boldsymbol{y}(x,t)+\boldsymbol{G}(x)\boldsymbol{u}(x,t)\tag{50}$$

$$\boldsymbol{y}_c(x,t)=\boldsymbol{C}(x)\boldsymbol{y}(x,t)\tag{51}$$

$$z(x,t)=\boldsymbol{H}(x)\boldsymbol{y}(x,t)+\boldsymbol{D}(x)u(x,t)\tag{52}$$

where $\xi=[\xi_1(y_1(x,t),x),\xi_2(y_1(x,t),x)]^T$ and $h_i(\xi)=w_i(\xi)/\sum_{i=1}^{4}w_i(\xi)$ $i\in\{1,2,3,4\}$ with

$$w_1(\xi)=F_{11}(\xi_1(y_1(x,t),x))F_{12}(\xi_2(y_1(x,t),x)),$$
$$w_2(\xi)=F_{21}(\xi_1(y_1(x,t),x))F_{12}(\xi_2(y_1(x,t),x)),$$

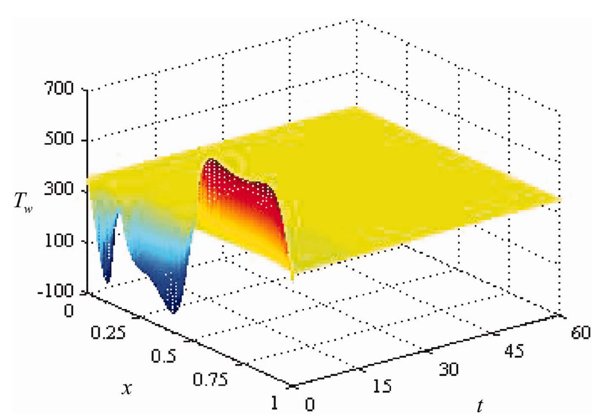

Figure 8. Closed-loop profile of evolution of jacket temperature.

[Color figure can be viewed in the online issue, which is available at wileyonlinelibrary.com.]

$$w_3(\xi)=F_{11}(\xi_1(y_1(x,t),x))F_{22}(\xi_2(y_1(x,t),x)),$$
$$w_4(\xi)=F_{21}(\xi_1(y_1(x,t),x))F_{22}(\xi_2(y_1(x,t),x)).$$

It is worth mentioning that the nonlinear PDE system of Eqs. 1–3 with parameters given in Eqs. 44 and 47 is represented by the T–S fuzzy PDE model in Eqs. 50–52, which is obtained by using the local sector nonlinearity method. The approximation error does not exist in the obtained fuzzy PDE model, as the local sector nonlinearity method can guarantee a locally exact fuzzy model construction under the condition $y_1(x,t)\in[\chi_{1e}(x)-\alpha,\chi_{1e}(x)+\alpha]$.

GCDF observer-based control design

In this subsection, we design the following fuzzy observer-based control law for the fuzzy PDE system of Eqs. 50–52:

$$\frac{\partial\hat{\boldsymbol{y}}(x,t)}{\partial t}=\boldsymbol{A}\hat{\boldsymbol{y}}(x,t)+\sum_{i=1}^{4}h_i(\xi)\boldsymbol{A}_i(x)\hat{\boldsymbol{y}}(x,t)+\boldsymbol{G}(x)\boldsymbol{u}(x,t)$$
$$+\sum_{i=1}^{r}h_i(\xi)\boldsymbol{L}_i(x)\boldsymbol{C}(x)[\boldsymbol{y}(x,t)-\hat{\boldsymbol{y}}(x,t)] \quad (53)$$

$$\boldsymbol{u}(x,t)=\sum_{i=1}^{4}h_i(\xi)\boldsymbol{K}_i(x)\hat{\boldsymbol{y}}(x,t) \quad (54)$$

where $\boldsymbol{K}_i(x)=\left[k_{i,1}(x),k_{i,2}(x)\right]$ and $\boldsymbol{L}_i(x)=\left[l_{i,1}(x),l_{i,2}(x)\right]^T$ $i\in\{1,2,3,4\}$ are 1×2 control gain matrices and 2×1 observer gain matrices to be determined, such that the resulting closed-loop fuzzy PDE system is exponentially stable and an optimized bound of the cost function in Eq. 15 is provided. Based on the result derived in section "GCDF Observer-Based Control Design," the outcome of the suboptimal GCDF observer-based control design for the system of Eqs. 50–52 is formulated as the SDLMI optimization problem in Eq. 27.

To implement the fuzzy controller of Eqs. 53 and 54, we use 80 equally distributed points along the reactor at which the temperature is observed and the coolant temperature is changed and thus $\varepsilon=0.0125$. Let $\boldsymbol{y}_0(x)=[0.15\sin(2\pi x)\quad -\chi_{2e}(x)]^T$ (i.e., the initial temperature is assumed to be $T_0(x)=T_{\text{in}}+0.15T_{\text{in}}\sin(2\pi x)$ and the initial reactant concentration is set to be $C_{A0}(x)=C_{A,\text{in}}$ for the original PFR model of Eqs. 36 and 37, $\boldsymbol{W}(x)=1$ $\eta=0.05$ and $\alpha=0.2$ By solving the LMI optimization problem in Eq. 35 via the *mincx* solver with the feasibility radius of 15, the optimized bound of cost function is obtained as $\rho^*=0.8785$ Using the resulting solutions $\boldsymbol{Q}_1(x_k)$ $\boldsymbol{Q}_2(x_k)$ $\boldsymbol{Z}_i(x_k)$ $\boldsymbol{N}_i(x_k)$ $i\in\mathcal{S}$ $k\in\mathcal{N}$ we can obtain the actual bound $J_b=\langle\boldsymbol{y}_0(\cdot),\boldsymbol{Q}_1^{-1}(\cdot)\boldsymbol{y}_0(\cdot)\rangle\approx0.6164$ and the corresponding observer and control gains $\boldsymbol{L}_i(x_k)$ $\boldsymbol{K}_i(x_k)$ $i\in\mathcal{S}$ $k\in\mathcal{N}$ as shown in Figures 2–5.

With above observer and control gains shown in Figures 2–5, we apply the fuzzy controller in Eqs. 53 and 54 to the PDE system of Eqs. 50–52. The actual closed-loop profiles of evolution of temperature, reactant concentration, and jacket temperature along the reactor are shown in Figures 6, respectively. It is observed from Figures 6–8 that when $t=60$, the temperature, reactant concentration of the inlet stream and jack temperature numerically converge to the chosen equilibrium profile. Then, we can obtain that the actual value of cost function in Eq. 15 with $\boldsymbol{W}(x)=1$ is 0.0844, that is, the suboptimal cost is ensured.

Conclusions

In this article, we have addressed the problem of GCDF observer-based control design for a class of nonlinear hyperbolic PDE systems. An SDLMI-based method for the GCDF observer-based control design has been developed on the basis of the T–S fuzzy PDE model. In the proposed design method, a distributed fuzzy observer is used to estimate the state of the PDE system, and a one-step design procedure is developed to obtain a suboptimal GCDF observer-based controller. The resulting controller can not only ensure the exponential stability of the closed-loop PDE system but also provide an optimized upper bound of quadratic cost function. Furthermore, using the finite difference method in space, the suboptimal control design problem is approximated by an LMI optimization problem, which can be efficiently solved by the standard LMI optimization techniques. Finally, the proposed design method is successfully applied to the control of a nonisothermal PFR, and the achieved simulation results show the effectiveness of the proposed controller.

Acknowledgments

This work was supported in part by the National Natural Science Foundation of China under Grants 61074057 and 61121003, in part by the National Basic Research Program of China (973 Program) (2011CB013104), in part by the Innovation Foundation of BUAA for PhD Graduates, and in part by the General Research Fund project from Research Grants Council of Hong Kong, SAR, under CityU: 116212. The authors also gratefully acknowledge the helpful comments and suggestions of the anonymous reviewers, which have improved the presentation.

Appendix: A
Proof of Theorem 1

Let us consider the following Lyapunov functional for the closed-loop PDE system of Eqs. 13 and 14

$$V(t)=\int_{z_1}^{z_2}\tilde{\boldsymbol{y}}^T(x,t)\boldsymbol{P}(x)\tilde{\boldsymbol{y}}(x,t)dx \quad (A1)$$

where $\boldsymbol{P}(x)>0$ $x\in[z_1,z_2]$ is a real continuous space-varying $2n\times2n$ matrix function. Differentiating $V(t)$ along the solution of the closed-loop system of Eqs. 13 and 14 yields

$$\frac{dV(t)}{dt}=\int_{z_1}^{z_2}\tilde{\boldsymbol{y}}^T(x,t)\boldsymbol{P}(x)\frac{\partial\tilde{\boldsymbol{y}}(x,t)}{\partial t}dx+\int_{z_1}^{z_2}\frac{\partial\tilde{\boldsymbol{y}}^T(x,t)}{\partial t}\boldsymbol{P}(x)\tilde{\boldsymbol{y}}(x,t)dx$$
$$=\int_{z_1}^{z_2}\left[\tilde{\boldsymbol{y}}^T(x,t)\boldsymbol{P}(x)\tilde{\boldsymbol{A}}\tilde{\boldsymbol{y}}(x,t)+\left(\tilde{\boldsymbol{A}}\tilde{\boldsymbol{y}}(x,t)\right)^T\boldsymbol{P}(x)\tilde{\boldsymbol{y}}(x,t)\right]dx$$
$$+\int_{z_1}^{z_2}\tilde{\boldsymbol{y}}^T(x,t)\left[\boldsymbol{P}(x)\tilde{\boldsymbol{A}}_c(\xi,x)+\tilde{\boldsymbol{A}}_c^T(\xi,x)\boldsymbol{P}(x)\right]\tilde{\boldsymbol{y}}(x,t)dx. \quad (A2)$$

By integrating by parts, we find that

$$\int_{z_1}^{z_2}\tilde{\boldsymbol{y}}^T(x,t)\boldsymbol{P}(x)\tilde{\boldsymbol{A}}\tilde{\boldsymbol{y}}(x,t)dx=\int_{z_1}^{z_2}\theta(x)\tilde{\boldsymbol{y}}^T(x,t)\boldsymbol{P}(x)\frac{\partial\tilde{\boldsymbol{y}}(x,t)}{\partial x}dx$$
$$=\theta(x)\tilde{\boldsymbol{y}}^T(x,t)\boldsymbol{P}(x)\tilde{\boldsymbol{y}}(x,t)|_{x=z_1}^{x=z_2}-\int_{z_1}^{z_2}\frac{\partial\left(\theta(x)\tilde{\boldsymbol{y}}^T(x,t)\boldsymbol{P}(x)\right)}{\partial x}\tilde{\boldsymbol{y}}(x,t)dx$$
$$=\theta(x)\tilde{\boldsymbol{y}}^T(x,t)\boldsymbol{P}(x)\tilde{\boldsymbol{y}}(x,t)|_{x=z_1}^{x=z_2}-\int_{z_1}^{z_2}\left(\tilde{\boldsymbol{A}}\tilde{\boldsymbol{y}}(x,t)\right)^T\boldsymbol{P}(x)\tilde{\boldsymbol{y}}(x,t)dx$$
$$-\int_{z_1}^{z_2}\tilde{\boldsymbol{y}}^T(x,t)\frac{d(\theta(x)\boldsymbol{P}(x))}{dx}\tilde{\boldsymbol{y}}(x,t)dx. \quad (A3)$$

We introduce the Dirac delta function $\delta(x)$, which is defined as follows[36]

$$\delta(x)=\begin{cases}0 & x\neq 0\\ \infty & x=0\end{cases} \text{ and } \int_{x_1}^{x_2}\delta(x)dx=1, \quad \text{if } 0\in[x_1,x_2]$$

with the fundamental property

$$\int_{x_1}^{x_2} f(x)\delta(x-x_0)dx=f(x_0), \quad x_0\in[x_1,x_2] \text{ for any function} f(x). \tag{A4}$$

Considering Eq. A3 and using the property in Eq. A4, we can obtain

$$\begin{aligned}&\int_{z_1}^{z_2}\left[\tilde{\boldsymbol{y}}^T(x,t)\boldsymbol{P}(x)\tilde{\boldsymbol{A}}\tilde{y}(x,t)+\left(\tilde{\boldsymbol{A}}\tilde{y}(x,t)\right)^T\boldsymbol{P}(x)\tilde{\boldsymbol{y}}(x,t)\right]dx\\ &=\int_{z_1}^{z_2}\tilde{\boldsymbol{y}}^T(x,t)\Psi(x)\tilde{\boldsymbol{y}}(x,t)dx.\end{aligned} \tag{A5}$$

where $\Psi(x)=-\frac{d}{dx}(\theta(x)\boldsymbol{P}(x))+[\delta(x-z_2)-\delta(x-z_1)]\theta(x)\boldsymbol{P}(x)$ Substitution of Eq. A5 into Eq. A2 gives

$$\begin{aligned}\frac{dV(t)}{dt}&=\int_{z_1}^{z_2}\tilde{\boldsymbol{y}}^T(x,t)\Psi(x)\tilde{\boldsymbol{y}}(x,t)dx\\ &+\int_{z_1}^{z_2}\tilde{\boldsymbol{y}}^T(x,t)\left[\boldsymbol{P}(x)\tilde{\boldsymbol{A}}_c(\xi,x)+\tilde{\boldsymbol{A}}_c^T(\xi,x)\boldsymbol{P}(x)\right]\tilde{\boldsymbol{y}}(x,t)dx\\ &=\int_{z_1}^{z_2}\tilde{\boldsymbol{y}}^T(x,t)\Theta(\xi,x)\tilde{\boldsymbol{y}}(x,t)dx\end{aligned} \tag{A6}$$

where $\Theta(\xi,x)=\Psi(x)+\boldsymbol{P}(x)\tilde{\boldsymbol{A}}_c(\xi,x)+\tilde{\boldsymbol{A}}_c^T(\xi,x)\boldsymbol{P}(x).$

On the other hand, from Eqs. 14 and A6, we have

$$\begin{aligned}&\frac{dV(t)}{dt}+\langle \boldsymbol{z}(\cdot,t),\boldsymbol{W}(\cdot)\boldsymbol{z}(\cdot,t)\rangle=\int_{z_1}^{z_2}\tilde{\boldsymbol{y}}^T(x,t)\\ &\left[\Theta(\xi,x)+\tilde{\boldsymbol{H}}_c^T(\xi,x)\boldsymbol{W}(x)\tilde{\boldsymbol{H}}_c(\xi,x)\right]\tilde{\boldsymbol{y}}(x,t)dx\end{aligned}$$

which implies

$$dV(t)/dt+\langle \boldsymbol{z}(\cdot,t),\boldsymbol{W}(\cdot)\boldsymbol{z}(\cdot,t)\rangle<0 \text{ for any nonzero } \tilde{\boldsymbol{y}}(\cdot,t)\in\mathscr{H}^{2n} \tag{A7}$$

if

$$\begin{aligned}&\int_{z_1}^{z_2}\tilde{\boldsymbol{y}}^T(x,t)\left[\Theta(\xi,x)+\tilde{\boldsymbol{H}}_c^T(\xi,x)\boldsymbol{W}(x)\tilde{\boldsymbol{H}}_c(\xi,x)\right]\tilde{\boldsymbol{y}}(x,t)dx\\ &<0 \text{ for any nonzero } \tilde{\boldsymbol{y}}(\cdot,t)\in\mathscr{H}^{2n}.\end{aligned} \tag{A8}$$

Obviously, the inequality in Eq. A8 is satisfied, if the following inequality holds for all $x\in[z_1,z_2]$

$$\Theta(\xi,x)+\tilde{\boldsymbol{H}}_c^T(\xi,x)\boldsymbol{W}(x)\tilde{\boldsymbol{H}}_c(\xi,x)<0. \tag{A9}$$

Now, we show that the inequality in Eq. A9 holds if both inequalities in Eqs. 16 and 17 are satisfied. By Schur complements,[32] the inequality in Eq. A9 is equivalent to the following inequality

$$\begin{bmatrix}\Theta(\xi,x) & \tilde{\boldsymbol{H}}_c^T(\xi,x)\\ \tilde{\boldsymbol{H}}_c(\xi,x) & -\boldsymbol{W}(x)\end{bmatrix}<0.$$

Using the definition of membership functions $h_i(\xi(x,t))$ $i\in\mathcal{S}$ and Eqs. A6, 6–8, 13, and 14, the above inequality can be written as

$$\sum_{i=1}^{r}\sum_{j=1}^{r}\bar{h}_{ij}(\xi(x,t))\tilde{\Theta}_{ij}(x)<0 \tag{A10}$$

where $\bar{h}_{ij}(\xi(x,t))=h_i(\xi(x,t))h_j(\xi(x,t))$ By Theorem 2.2,[25] we can conclude that the inequality in Eq. A10 holds if both inequalities in Eqs. 16 and 17 hold. Hence, from above analysis, it follows that the inequality in Eq. A7 holds if both inequalities in Eqs. 16 and 17 hold for all $x\in[z_1,z_2]$. We will show that the closed-loop system of Eqs. 13 and 14 is exponentially stable if the inequality in Eq. A7 holds.

From the inequality in Eq. A9, we can find an appropriate scalar $p_2>0$ such that

$$\Theta(\xi,x)+\tilde{\boldsymbol{H}}_c^T(\xi,x)\boldsymbol{W}(x)\tilde{\boldsymbol{H}}_c(\xi,x)+p_2\boldsymbol{I}\leq 0$$

which implies that the inequality in Eq. A7 can be rewritten as

$$dV(t)/dt\leq -p_2\|\tilde{\boldsymbol{y}}(\cdot,t)\|_2^2 \text{ for any nonzero } \tilde{\boldsymbol{y}}(\cdot,t)\in\mathscr{H}^{2n} \tag{A11}$$

As $\boldsymbol{P}(x)>0$ $x\in[z_1,z_2]$ is a spatially continuous matrix function, it is easily observed that $V(t)$ given by Eq. A1 satisfies the inequality

$$\tau_1\|\tilde{\boldsymbol{y}}(\cdot,t)\|_2^2\leq V(t)\leq\tau_2\|\tilde{\boldsymbol{y}}(\cdot,t)\|_2^2 \tag{A12}$$

where $\tau_1=\min_{x\in[z_1,z_2]}\{\lambda_{\min}(\boldsymbol{P}(x))\}$ and $\tau_2=\max_{x\in[z_1,z_2]}\{\lambda_{\max}(\boldsymbol{P}(x))\}$ are two positive constants. Inequalities in Eqs. A11 and A12 imply that for any nonzero $\tilde{\boldsymbol{y}}(\cdot,t)\in\mathscr{H}^{2n}$,

$$dV(t)/dt\leq -p_2\tau_2^{-1}V(t). \tag{A13}$$

Integration of the inequality in Eq. A13 from zero to t gives

$$V(t)\leq V(0)\exp\left(-p_2\tau_2^{-1}t\right). \tag{A14}$$

From Eqs. A12 and A14, we have

$$\|\tilde{\boldsymbol{y}}(\cdot,t)\|_2^2\leq\tau_2\tau_1^{-1}\|\tilde{\boldsymbol{y}}_0(\cdot)\|_2^2\exp\left(-p_2\tau_2^{-1}t\right).$$

Thus, by Definition , the closed-loop PDE system of Eqs. 13 and 14 is exponentially stable, which means $\|\tilde{\boldsymbol{y}}(\cdot,t)\|_2^2\to 0$ as $t\to\infty$ Therefore, using Eq. 15, rearranging, and integrating the inequality in Eq. A7 from zero to infinity, we have

$$J=\int_0^\infty\langle \boldsymbol{z}(\cdot,t),\boldsymbol{W}(\cdot)\boldsymbol{z}(\cdot,t)\rangle dt<-V(t)|_{t=0}^{t=\infty}=\langle\tilde{\boldsymbol{y}}_0(\cdot),\boldsymbol{P}(\cdot)\tilde{\boldsymbol{y}}_0(\cdot)\rangle,$$

which implies

$$J<\langle\tilde{\boldsymbol{y}}_0(\cdot),\boldsymbol{P}(\cdot)\tilde{\boldsymbol{y}}_0(\cdot)\rangle. \tag{A15}$$

From Eq. A15, we have Eq. 18. ■

Appendix: B

Proof of Theorem 2

Necessity

First suppose that the inequalities in Eqs. 16 and 17 have a set of feasible solutions $\boldsymbol{P}(x)>0$ $\boldsymbol{K}_i(x)$ and $\boldsymbol{L}_i(x)$ $i\in\mathcal{S}$. With $\boldsymbol{P}(x)$ partitioned as $n\times n$ blocks

$$\boldsymbol{P}(x)=\begin{bmatrix}\boldsymbol{P}_{11}(x) & \boldsymbol{P}_{12}(x)\\ \boldsymbol{P}_{12}^T(x) & \boldsymbol{P}_{22}(x)\end{bmatrix}, \tag{B1}$$

we easily check that inequalities in Eqs. 16 and 17 imply

$$\bar{\Phi}_{1,ii}(x)<0,\quad i\in\mathcal{S} \tag{B2}$$

$$\frac{1}{r-1}\bar{\Phi}_{1,ii}(x)+\frac{1}{2}\left(\bar{\Phi}_{1,ij}(x)+\bar{\Phi}_{1,ji}(x)\right)<0,\quad i\neq j,\quad i,j\in\mathcal{S} \tag{B3}$$

where

$$\bar{\Phi}_{1,ij}(x)=\begin{bmatrix}\bar{\Psi}_{11,ij}(x) & \boldsymbol{H}_{c,ij}^T(x)\\ \boldsymbol{H}_{c,ij}(x) & -\boldsymbol{W}^{-1}(x)\end{bmatrix},\quad i,j\in\mathcal{S},$$

with

$$\bar{\Psi}_{11,ij}(x)=\boldsymbol{P}_{11}(x)\boldsymbol{A}_{c,ij}(x)+\boldsymbol{A}_{c,ij}^T(x)\boldsymbol{P}_{11}(x)$$
$$-\frac{d}{dx}(\theta(x)\boldsymbol{P}_{11}(x))+[\delta(x-z_2)-\delta(x-z_1)]\theta(x)\boldsymbol{P}_{11}(x).$$

Let

$$\boldsymbol{Q}_1(x)=\boldsymbol{P}_{11}^{-1}(x)\text{and}\,\boldsymbol{N}_i(x)=\boldsymbol{K}_i(x)\boldsymbol{Q}_1(x), i\in\mathcal{S}. \tag{B4}$$

Premultiplying and postmultiplying the inequalities in Eqs. B2 and B3 by matrix diag $\{\boldsymbol{Q}_1(x),\boldsymbol{I}\}$ respectively, and using the following property

$$\frac{d\boldsymbol{Q}_1(x)}{dx}=-\boldsymbol{Q}_1(x)\frac{d\boldsymbol{Q}_1^{-1}(x)}{dx}\boldsymbol{Q}_1(x). \tag{B5}$$

the inequalities in Eqs. B2 and B3 is equivalent to the SDLMIs in Eqs. 19 and 20.

Define $\boldsymbol{Q}(x)=\boldsymbol{P}^{-1}(x)$ Using Eq. B5 with $\boldsymbol{Q}_1(x)=\boldsymbol{Q}(x)$ the inequalities in Eqs. 16 and 17 become

$$\bar{\Phi}_{ii}(x)<0,\quad i\in\mathcal{S} \tag{B6}$$

$$\frac{1}{r-1}\bar{\Phi}_{ii}(x)+\frac{1}{2}\left(\bar{\Phi}_{ij}(x)+\bar{\Phi}_{ji}(x)\right)<0,\quad i\neq j,\quad i,j\in\mathcal{S} \tag{B7}$$

where

$$\bar{\Phi}_{ij}(x)=\begin{bmatrix}\bar{\Psi}_{ij}(x) & \boldsymbol{Q}(x)\tilde{\boldsymbol{H}}_{c,ij}^T(x)\\ \tilde{\boldsymbol{H}}_{c,ij}(x)\boldsymbol{Q}(x) & -\boldsymbol{W}^{-1}(x)\end{bmatrix},\quad i,j\in\mathcal{S}$$

with

$$\bar{\Psi}_{ij}(x)=\tilde{\boldsymbol{A}}_{c,ij}(x)\boldsymbol{Q}(x)+\boldsymbol{Q}(x)\tilde{\boldsymbol{A}}_{c,ij}^T(x)+\theta(x)\frac{d\boldsymbol{Q}(x)}{dx}-\frac{d\theta(x)}{dx}\boldsymbol{Q}(x)$$
$$+[\delta(x-z_2)-\delta(x-z_1)]\theta(x)\boldsymbol{Q}(x).$$

By partitioning $\boldsymbol{Q}(x)$ as $n\times n$ blocks

$$\boldsymbol{Q}(x)=\begin{bmatrix}\boldsymbol{Q}_{11}(x) & \boldsymbol{Q}_{12}(x)\\ \boldsymbol{Q}_{12}^T(x) & \boldsymbol{Q}_{22}(x)\end{bmatrix},$$

we easily check that the inequalities in Eqs. B6 and B7 imply

$$\bar{\Phi}_{2,ii}(x)<0,\quad i\in\mathcal{S} \tag{B8}$$

$$\frac{1}{r-1}\bar{\Phi}_{2,ii}(x)+\frac{1}{2}\left(\bar{\Phi}_{2,ij}(x)+\bar{\Phi}_{2,ji}(x)\right)<0,\quad i\neq j,\quad i,j\in\mathcal{S} \tag{B9}$$

where

$$\begin{aligned}\bar{\Phi}_{2,ij}(x)=&\boldsymbol{A}_i(x)\boldsymbol{Q}_{22}(x)+\boldsymbol{Q}_{22}(x)\boldsymbol{A}_i^T(x)-\boldsymbol{L}_i(x)\boldsymbol{C}_j(x)\boldsymbol{Q}_{22}(x)\\ &-\boldsymbol{Q}_{22}(x)\boldsymbol{C}_j^T(x)\boldsymbol{L}_i^T(x)+\theta(x)\frac{d\boldsymbol{Q}_{22}(x)}{dx}-\frac{d\theta(x)}{dx}\boldsymbol{Q}_{22}(x)\\ &+[\delta(x-z_2)-\delta(x-z_1)]\theta(x)\boldsymbol{Q}_{22}(x)+\theta(x)\frac{d\boldsymbol{Q}_{22}(x)}{dx}\\ &-\frac{d\theta(x)}{dx}\boldsymbol{Q}_{22}(x)+[\delta(x-z_2)-\delta(x-z_1)]\theta(x)\boldsymbol{Q}_{22}(x).\end{aligned}$$

Let

$$\boldsymbol{Q}_2(x)=\boldsymbol{Q}_{22}^{-1}(x)\text{and}\,\boldsymbol{Z}_i(x)=\boldsymbol{Q}_2(x)\boldsymbol{L}_i(x),\quad i\in\mathcal{S}. \tag{B10}$$

Premultiplying and postmultiplying the inequalities in Eqs. B8 and B9 by the matrix $\boldsymbol{Q}_2(x)$ respectively, and using Eq. B5 with $\boldsymbol{Q}_1(x)=\boldsymbol{Q}_2(x)$ the inequalities in Eqs. B8 and B9 are equivalent to the SDLMIs in Eqs. 21 and 22. From Eqs. B4 and B10, we have Eq. 24.

Sufficiency

Suppose that $\boldsymbol{Q}_1(x)>0$ $\boldsymbol{Q}_2(x)>0$ $\boldsymbol{N}_i(x)$ $\boldsymbol{Z}_i(x)$ $i\in\mathcal{S}$ satisfy the SDLMIs in Eqs. 19–22 and define $\boldsymbol{K}_i(x)$ and $\boldsymbol{L}_i(x)$ as Eq. 24. Using Eq. B5, we can see that Eqs. 19 give

$$\Xi_{1,ii}(x)<0,\quad i\in\mathcal{S} \tag{B11}$$

$$\frac{1}{r-1}\Xi_{1,ii}(x)+\frac{1}{2}\left(\Xi_{1,ij}(x)+\Xi_{1,ji}(x)\right)<0,\quad i\neq j,\quad i,j\in\mathcal{S} \tag{B12}$$

$$\Xi_{2,ii}(x)<0,\quad i\in\mathcal{S} \tag{B13}$$

$$\frac{1}{r-1}\Xi_{2,ii}(x)+\frac{1}{2}\left(\Xi_{2,ij}(x)+\Xi_{2,ji}(x)\right)<0,\quad i\neq j,\quad i,j\in\mathcal{S} \tag{B14}$$

where

$$\Xi_{1,ij}(x)=\begin{bmatrix}\Xi_{11,ij}(x) & \boldsymbol{H}_{c,ij}^T(x)\\ \boldsymbol{H}_{c,ij}(x) & -\boldsymbol{W}^{-1}(x)\end{bmatrix},\quad i,j\in\mathcal{S}$$

$$\begin{aligned}\Xi_{2,ij}(x)=&\boldsymbol{Q}_2(x)\boldsymbol{A}_i(x)+\boldsymbol{A}_i^T(x)\boldsymbol{Q}_2(x)-\boldsymbol{Q}_2(x)\boldsymbol{L}_i(x)\boldsymbol{C}_j(x)\\ &-\boldsymbol{C}_j^T(x)\boldsymbol{L}_i^T(x)\boldsymbol{Q}_2(x)-\frac{d}{dx}(\theta(x)\boldsymbol{Q}_2(x))\\ &+[\delta(x-z_2)-\delta(x-z_1)]\theta(x)\boldsymbol{Q}_2(x), i,j\in\mathcal{S}\end{aligned}$$

with

$$\begin{aligned}\Xi_{11,ij}(x)=&\boldsymbol{Q}_1^{-1}(x)\boldsymbol{A}_{c,ij}(x)+\boldsymbol{A}_{c,ij}^T(x)\boldsymbol{Q}_1^{-1}(x)-\frac{d}{dx}\left(\theta(x)\boldsymbol{Q}_1^{-1}(x)\right)\\ &+[\delta(x-z_2)-\delta(x-z_1)]\theta(x)\boldsymbol{Q}_1^{-1}(x).\end{aligned}$$

By Schur complement,[32] it follows from Eqs. B11 that there exists a scalar $\chi_0>0$ such that

$$\Xi_{ii}(x)<0,\quad i\in\mathcal{S} \tag{B15}$$

$$\frac{1}{r-1}\Xi_{ii}(x)+\frac{1}{2}\left(\Xi_{ij}(x)+\Xi_{ji}(x)\right)<0,\quad i\neq j,\quad i,j\in\mathcal{S} \tag{B16}$$

holds for all $x\in[z_1,z_2]$ and any $\chi\geq\chi_0$ where

$$\Xi_{ij}(x)=\begin{bmatrix}\Xi_{1,ij}(x) & \Xi_{3,ij}(x)\\ \Xi_{3,ij}^T(x) & \chi\Xi_{2,ij}(x)\end{bmatrix},$$

$$\Xi_{3,ij}(x)=\begin{bmatrix}-\boldsymbol{K}_i^T(x)\boldsymbol{G}_j^T(x)\boldsymbol{Q}_1^{-1}(x) & -\boldsymbol{K}_i^T(x)\boldsymbol{D}_j^T(x)\end{bmatrix}^T.$$

Exchanging rows and columns of Eqs. B15 and B16, yields exactly Eqs. 16 and 17 with $\boldsymbol{P}(x) = \operatorname{diag}\left\{\boldsymbol{Q}_1^{-1}(x), \chi\boldsymbol{Q}_2(x)\right\} > 0$ for any $\chi \geq \chi_0$.

Moreover, by considering Eq. B1 and $\tilde{\boldsymbol{y}}_0(x) = \left[\boldsymbol{y}_0^T(x)\ 0\right]^T$ the inequality in Eq. 18 can be represented as

$$J < J_b = \langle \tilde{\boldsymbol{y}}_0(\cdot), \boldsymbol{P}(\cdot)\tilde{\boldsymbol{y}}_0(\cdot)\rangle = \langle \boldsymbol{y}_0(\cdot), \boldsymbol{P}_{11}(\cdot)\boldsymbol{y}_0(\cdot)\rangle. \tag{B17}$$

Hence, we can obtain Eq. 23 from Eqs. B4 and B17. ■

Literature Cited

1. Ray WH. Advanced Process Control. New York: McGraw-Hill, 1981.
2. Christofides PD. Nonlinear and Robust Control of PDE Systems: Methods and Applications to Transport-Reaction Processes. Boston, MA: Birkhäuser, 2001.
3. Li HX, Qi C. Modeling of distributed parameter systems for applications—a synthesized review from time-space separation. *J Process Control.* 2010;20:891–901.
4. Balas MJ. Feedback control of linear diffusion processes. *Int J Control.* 1979;29:523–534.
5. Curtain RF. Finite-dimensional compensator design for parabolic distributed systems with point sensors and boundary input. *IEEE Trans Automat Control.* 1982;27:98–104.
6. Balas MJ. The Galerkin method and feedback control of linear distributed parameter systems. *J Math Anal Appl.* 1983;91:527–546.
7. Christofides PD, Daoutidis P. Finite-dimensional control of parabolic PDE systems using approximate inertial manifolds. *J Math Anal Appl.* 1997;216:398–420.
8. Baker J, Christofides PD. Finite-dimensional approximation and control of nonlinear parabolic PDE systems. *Int J Control.* 2000;73:439–456.
9. Hagen G, Mezic I. Spillover stabilization in finite-dimensional control and observer design for dissipative evolution equations. *SIAM J Control Optim.* 2003;42:746–768.
10. Chen BS, Chang YT. Fuzzy state-space modeling and robust observer-based control design for nonlinear partial differential systems. *IEEE Trans Fuzzy Syst.* 2009;17:1025–1043.
11. El-Farra NH, Ghantasala S. Actuator fault isolation and reconfiguration in transport-reaction processes. *AIChE J.* 2007;53:1518–1537.
12. Wu HN, Li HX. H_∞ fuzzy observer-based control for a class of nonlinear distributed parameter systems with control constraints. *IEEE Trans Fuzzy Syst.* 2008;16:502–516.
13. Curtain RF, Zwart HJ. An Introduction to Infinite-Dimensional Linear Systems Theory. New York: Springer-Verlag, 1995.
14. Aksikas I, Fusman A, Forbes JF, Winkin JJ. LQ control design of a class of hyperbolic PDE systems: application to fixed-bed reactor. *Automatica.* 2009;45:1542–1548.
15. Hanczyc EM, Palazoglu A. Sliding mode control of nonlinear distributed parameter processes. *Ind Eng Chem Res.* 1995;34:557–566.
16. Christofides PD, Daoutidis P. Feedback control of hyperbolic PDE systems. *AIChE J.* 1996;42:3063–3086.
17. Christofides PD, Daoutidis P. Robust control of hyperbolic PDE systems. *Chem Eng Sci.* 1998;53:85–105.
18. Shang H, Forbes JF, Guay M. Model predictive control for quasilinear hyperbolic distributed parameter systems. *Ind Eng Chem Res.* 2004;43:2140–2149.
19. Dubljevic S, Mhaskar P, El-Farra NH, Christofides, PD. Predictive control of transport-reaction processes. *Comput Chem Eng.* 2005;29:2335–2345.
20. Choi J, Lee KS. Model predictive control of cocurrent first-order hyperbolic PDE systems. *Ind Eng Chem Res.* 2005;44:1812–1822.
21. Takagi T, Sugeno M. Fuzzy identification of systems and its applications to modeling and control. *IEEE Trans Syst Man Cybern.* 1985;15:116–132.
22. Tanaka K, Wang HO. Fuzzy Control Systems Design and Analysis: A Linear Matrix Inequality Approach. New York: Wiley, 2001.
23. Feng G. Analysis and Synthesis of Fuzzy Control Systems: A Model Based Approach. Boca Raton, FL: CRC, 2010.
24. Precup RE, Hellendoorn H. A survey on industrial applications of fuzzy control. *Comput Ind.* 2011;62:213–226.
25. Tuan HD, Apkarian P, Narikiyo T, Yamamoto Y. Parameterized linear matrix inequality techniques in fuzzy control system design. *IEEE Trans Fuzzy Syst.* 2001;9:324–332.
26. Chen B, Liu X. Fuzzy guaranteed cost control for nonlinear systems with time-varying delay. *IEEE Trans Fuzzy Syst.* 2005;13:238–249.
27. Zhang HG, Wang Y, Liu D. Delay-dependent guaranteed cost control for uncertain stochastic fuzzy systems with multiple time delays. *IEEE Trans Syst Man Cybern B Cybern.* 2008;38:126–140.
28. Wu HN. An ILMI approach to robust H_2 static output feedback fuzzy control for uncertain discrete-time nonlinear systems. *Automatica.* 2008;44:2333–2339.
29. Lima NMN, Linan LZ, Filho RM, Maciel MRW, Embirucu M, Gracio F. Modeling and predictive control using fuzzy logic: application for a polymerization system. *AIChE J.* 2010;56:965–978.
30. Dong H, Wang Z, Ho DWC, Gao H. Robust H_∞ fuzzy output-feedback control with multiple probabilistic delays and multiple missing measurements. *IEEE Trans Fuzzy Syst.* 2010;18:712–725.
31. Wang JW, Wu HN, Li HX. Distributed fuzzy control design of nonlinear hyperbolic PDE systems with application to nonisothermal plug-flow reactor. *IEEE Trans Fuzzy Syst.* 2011;19:514–526.
32. Boyd S, Ghaoui LE, Feron E, Balakrishnan V. Linear Matrix Inequalities in System and Control Theory. Philadelphia, PA: SIAM, 1994.
33. Gahinet P, Nemirovskii A, Laub AJ, Chilali M. LMI Control Toolbox for Use with Matlab. Natick MA: The MathWorks, Inc., 1995.
34. Bamieh B, Paganini F, Dahleh MA. Distributed control of spatially invariant systems. *IEEE Trans Automat Control.* 2002;47:1091–1107.
35. Demetriou MA. Guidance of mobile actuator-plus-sensor networks for improved control and estimation of distributed parameter systems. *IEEE Trans Automat Control.* 2010;55:1570–1584.
36. Levine IN. Quantum Chemistry, 6th ed. NJ: Pearson Prentice Hall, 2009.
37. Toker O, Ozbay H. On the NP-hardness of solving bilinear matrix inequalities and simultaneous stabilization with static output feedback. In: Proceedings of the 1995 American Control Conference, Seattle, WA; IEEE: Piscataway (NJ), USA, 1995:2525–2526.
38. Burden RL, Faires JD. Numerical Analysis, 7th ed. New York: Brooks/Cole, 2000.

Manuscript received Feb. 20, 2012, revision received Jun. 11, 2012, and final revision received Dec. 13, 2012.